IX Latin American Rock Mechanics Symposium
IX Simposio Latinoamericano de Mecánica de Rocas
Asunción-Paraguay
October 16-19, 2022 *KEYNOTE PAPERS*

Keynote Lecture: Continuum or Discontinuum – That is the Question

N.R. Barton
Nick Barton and Associates, Oslo, Norway

ABSTRACT:

Several decades ago there was a strong focus on the need for discontinuum modelling to improve upon the empirically based analysis of excavations in jointed rock. The remarkable codes developed by Peter Cundall: UDEC and 3DEC were put to full use in the nineteen eighties and nineties. For example, Q-system based cavern support could be verified or improved with such analyses. Of course, these codes preferably require knowledge of rock mechanics and rock joint behaviour, and perhaps familiarity with non-linear constitutive models as in UDEC-BB. Regrettably the classic textbooks of Hoek and Bray and Hoek and Brown in this period were subsequently followed by the suggestions for continuum modelling using a still not finalized GSI – there are many attempts at improved quantification. JRC now reaching 50 years is also the subject of improved quantification, but it is not followed by the extraordinary page-wide equations for 'c' and 'φ' so no software is needed. The incorrect addition of these components of shear strength (as indeed in Mohr-Coulomb) in commercial continuum codes is the final source of error of so many analyses. So-called plastic zones are exaggerated around tunnels, and rock slopes are given seldom observed deep spoon-shaped failure predictions, ignoring the frequent influence of major discontinuities, and the usual failures within the slope faces. Of course, lake-bed open-pit slope deposits or extremely weathered rock will give spoon-shaped failures as for rockfill and soil, but competent jointed rock will not fail like this: major discontinuities will usually be involved, and wedge or planar failures will be the usual reality.

1 INTRODUCTION

We were advised more than 50 years ago by Brace and Müller that cohesion is broken before friction is fully mobilized. Gross errors are caused by adding these components of shear strength when estimating the maximum height of cliffs and mountain walls. Since 'c' is not the lowest component of strength, artificially lowered estimates are needed, or tensile strength and Poisson's ratio are used (Barton and Shen, 2017). There is precious little empirical basis for the Hoek-Brown equations for rock mass strength, but an excellent experimental basis of course for the earlier intact rock H-B criterion. We may ask if is it logical to downgrade the strength of intact rock to model rock masses (using opaque equations with joint roughness and number of joint sets ignored) or better to apply the equations for the shear strength of joints and fractures and estimate the initial cohesive contribution of intact bridges between the kinematically capable joint sets? In this lecture the author will be showing studies with UDEC, 3DEC, FLAC and FLAC3D and FRACOD, and will be illustrating both discontinuum and continuum analyses for tunnels, caverns and open-pit slopes. An earlier than UDEC phase, with fractured (2D) models of underground excavations, will also be shown as an introduction.

2 PHYSICAL MODELS WITH FRACTURES PRE UDEC

The author was a student colleague of Cundall while he started to develop his first remarkable computer code with blocks. However, we may start with what could be achieved with physical

models of fractured media *before Cundall's codes became available,* both pre-1970 and from just prior to the Cundall/Itasca UDEC release in 1980. He was inspired to do better, as in Fig. 1.

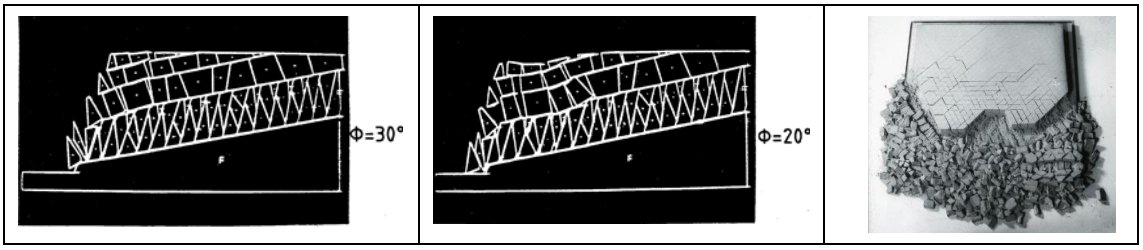

Figure 1. The contrasting flexibility of Cundall's intelligent computer code µDEC: two of four results of varying angle φ from Cundall et al. (1975). A big contrast to the 'fixed-fracture-sets' fractured 2D models developed some years earlier by the author in 1968. These physical models were utilized on two occasions before UDEC was released. Several 2D 'slab models' with carefully loaded and excavated slope models of 40,000 blocks were followed some years later with underground opening models with 20,000 blocks (Figs 2, 3 & 4). Individual slab models also allowed investigation of the relative effects of 4,000, 1,000 and 250 blocks in biaxial loading, which assisted in block-size scale effect understanding. The smallest block sizes gave unexpected 'linear' stress-strain behaviour and some kink-band modes.

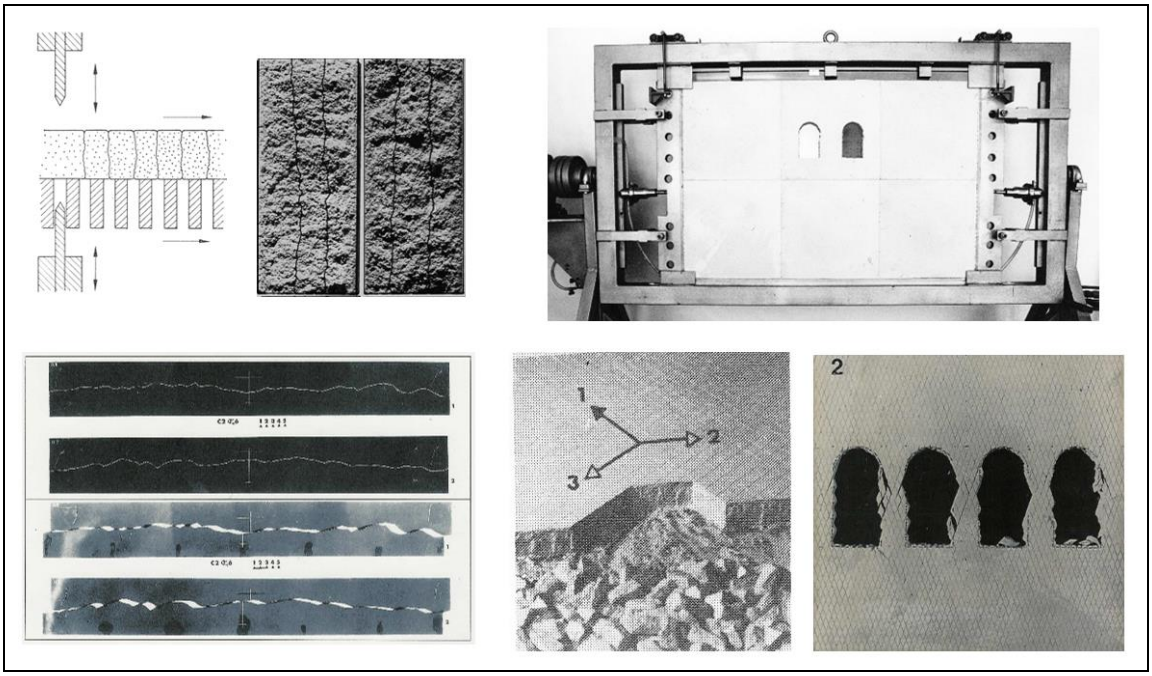

Figure 2. The principal mechanism of tension-fracture development and their roughness are illustrated top left. A subsequent physical model series reported by Barton & Hansteen (1979) is shown on the right. (My NGI colleague provided the continuum model comparisons). One year after publication of these UNPP (underground nuclear power plant) studies, UDEC became commercially available. No regrets.

Some of these early pre-UDEC physical fracture models are reproduced in this lecture as they still appear not to have been repeated by others and represent a 'physical reality' even though not a 'geological reality'. They may serve as 2D code verification objects. In the end the early UNPP studies in Norway including site characterization, came to nothing, and Sweden (who had part-funded these physical model studies through BeFo) built surface nuclear plants, while Norway continued with more extensive underground hydroelectric power developments.

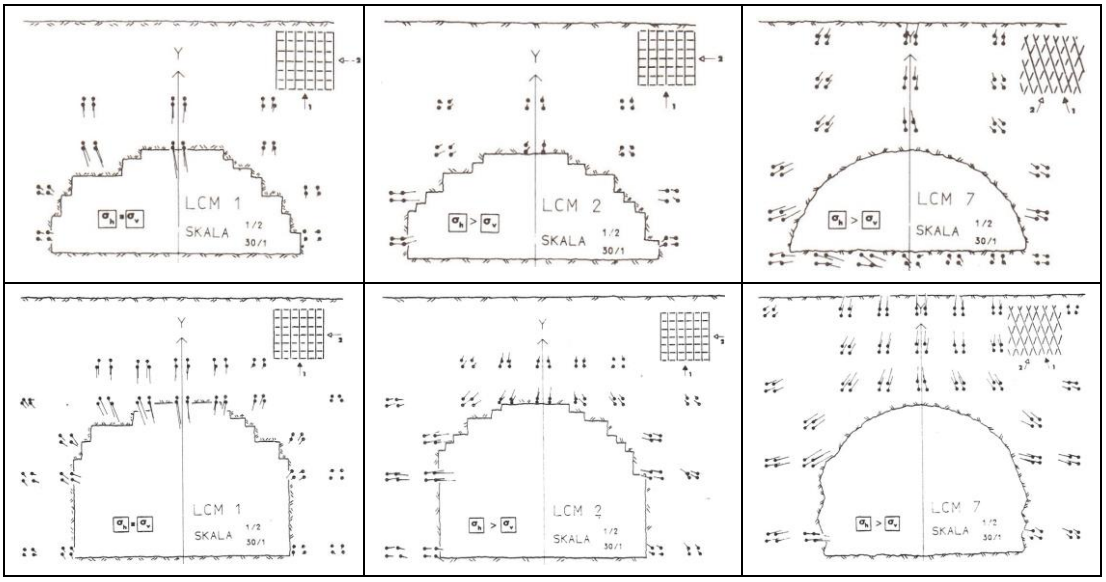

Figure 3. A selection of the cavern models which were studied in the pre-UDEC period, in order to evaluate the feasibility of underground nuclear power plant (UNPP) spans of 50m. The deformation vectors show the importance of horizontal stress and demonstrate the inevitable inadequacy of isotropic continuum modelling. The inset joint (fracture) structures are at correct scale and show primary and secondary fracture sets. All models had 20,000 blocks, meaning distant boundaries. Barton & Hansteen (1979).

3 SOME FUNDAMENTALS OF JOINT BEHAVIOUR

The physical fracture models suggested significant differences to continuum modelling, with joint orientations being particularly important. In Figure 4 we can also see a more fundamental feature of joint behavior. The four caverns were excavated one after the other in a high horizontal stress situation, as in four of the cases in Figure 3. Of particular note is the hysteresis or 'deformation set' seen in the narrow pillars. The photogrammetry-determined deformations did not reverse noticeably, when a new cavern was excavated, as would have happened in an elastic continuum model.

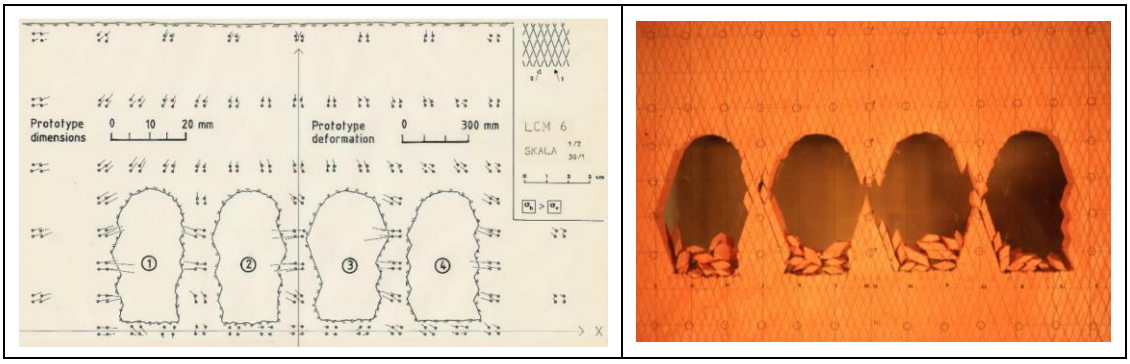

Figure 4. A multi-cavern experiment with ultra-narrow pillars, prior to model earthquake loading monitored with an accelerometer (giving a scaled 0.1 to 0.7g). Note the hysteresis in the cavern pillars. No reversal of deformations with successive cavern excavation. Fracture roughness and dilation explain the apparent tensile strength. Note that primary (continuous) fracture set #1 dips to the right, and has no

cohesive strength, just very high dilation and total friction angles at low normal stress. (Barton, 1973). Figure 2, bottom right, shows the cavern degradation progress during the model 'earthquake'.
In the next figure we see that three basic styles of rock mass deformation may occur with jointed rock masses, and each have been recorded by large scale *in situ* loading tests. They are clearly absent from conventional continuum modelling.

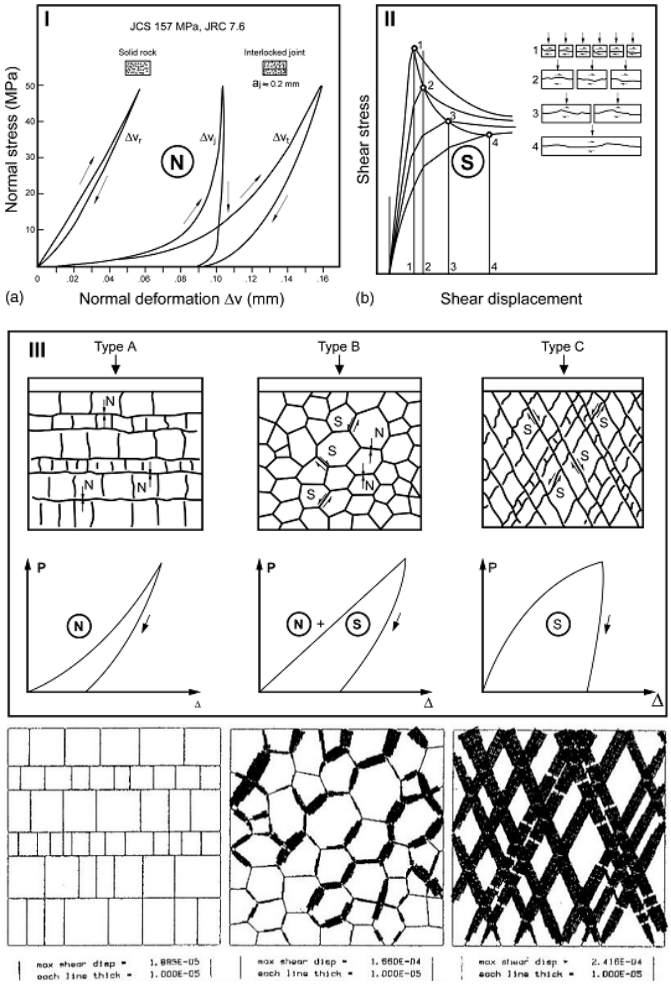

Figure 5. The N (normal) Type A concave deformation and the S (shear) Type C convex deformation, with the combined mode Type B as seen in loading tests across columnar basalt. Chryssanthakis et al. (1991) matched these three styles of deformation using UDEC-BB after this code became available in 1985. Note the normal stress-closure curves from Bandis et al. (1983) and the shear stress-displacement curves (with scale effects) from Bandis et al. (1981). The N and S and N+S load-deformation trends and the three rock mass assemblies are from Barton (1986).

To state the obvious there are no continuum model or GSI-based Hoek-Brown equations to match the essentially discontinuous behaviour shown in any of the previous figures, nor the shear strength details seen in Figure 6. GSI users can perhaps be happy that their 'rock engineering' activities are significantly easier thanks to RocScience software. But was the practice of rock mechanics for rock engineering supposed to be so easy? In the opinion of the author the use of GSI and continuum models has taken the realism out of the subject, which was not the original intention of Hoek and Bray and Hoek and Brown. These were classically helpful textbooks that also addressed discontinuum behaviour, the first one especially so.

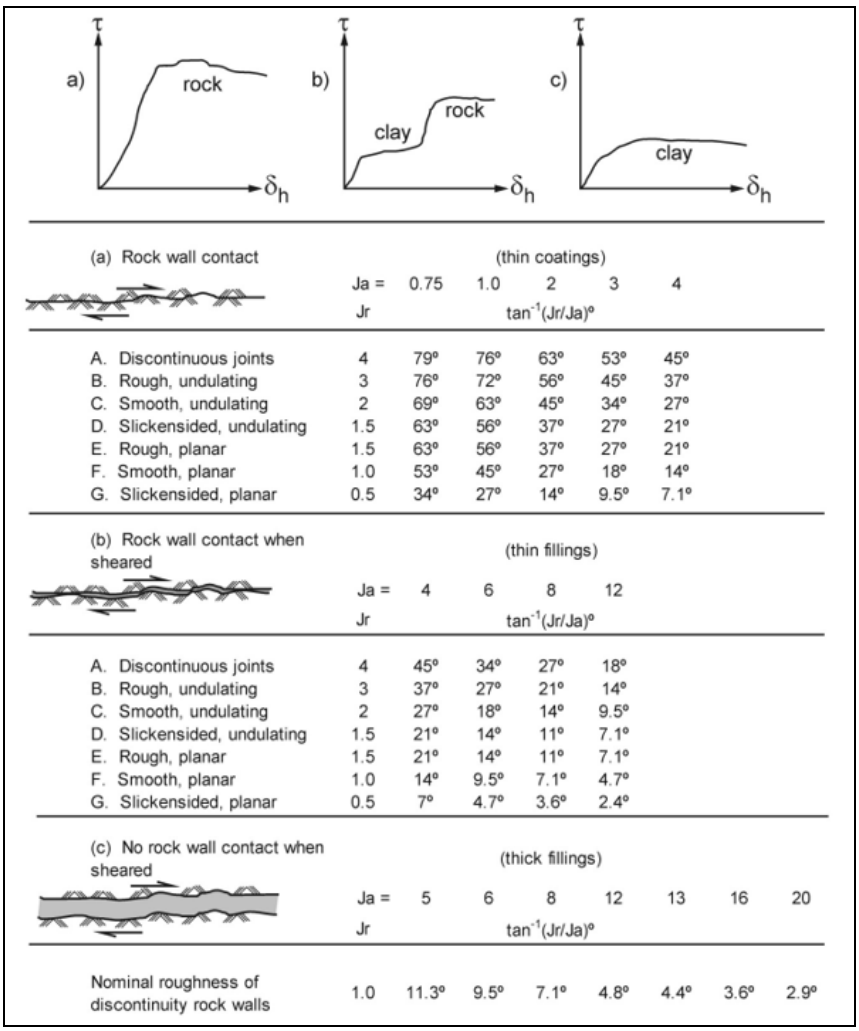

Figure 6. Variations in the shear strength of unfilled, clay-coated, and clay-filled discontinuities as illustrated here from the two Q-system parameters Jr/Ja cannot be included in GSI in a 'free manner' independent of joint roughness, because the GSI use of Bieniawski's joint condition factor (along the x-axis) does not make such differentiation possible. The Bieniawski (1989) 'joint condition' moves in one direction, so rougher joints cannot have clay coatings or fillings, and even more remarkably: slickensides must be weathered. Figure from Barton (2002).

4 SOME EXAMPLES OF UDEC-BB MODELS SHOWING GEOLOGICAL DETAIL

In the following rather concentrated selection of discontinuum models the author will show features of potential behaviour that can hardly be matched by continuum modelling. The exception – to a degree – is the redistribution of stress, from principle far-field stresses to tangential and radial stresses. The rotation of the small 'crosses' are of course seen clearly in continuum models, but the loading of bolts where they cross and support wedges, and the unstressed unstable wedges are not seen in continuum models. The discontinuum model teaches us to look out for important behaviour that is absent from continuum modelling. In UDEC-BB we see the distribution of joint shearing and also the stress- or depth-dependent physical apertures, and JRC-estimated hydraulic apertures, for coupled H-M modelling. An introductory set of results with input is shown in Fig. 7.

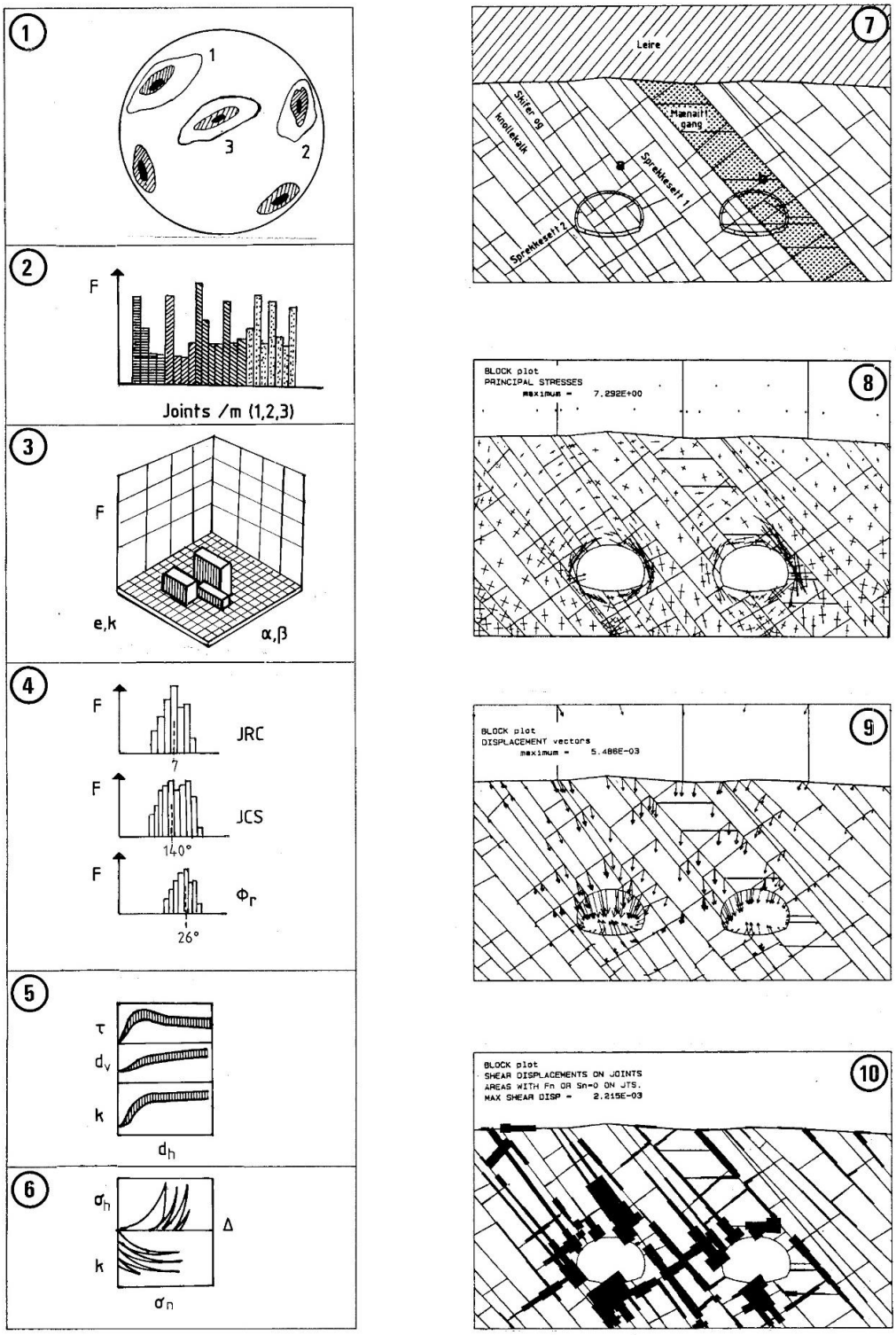

Figure 7. A glimpse of the principles of discontinuum modelling input data operations as applying to UDEC-BB. On the left: joint orientations and frequencies, permeability and aperture estimation (but this will be estimated by UDEC-BB) and joint index test results for JRC, JCS and φ_r. Boxes 5 and 6 symbolize the shear stress-displacement-dilation-permeability and normal stress-closure operations of the Barton-Bandis model. (See Barton et al., 1985, Barton, 1993 and Barton and Bandis, 2017 for examples).

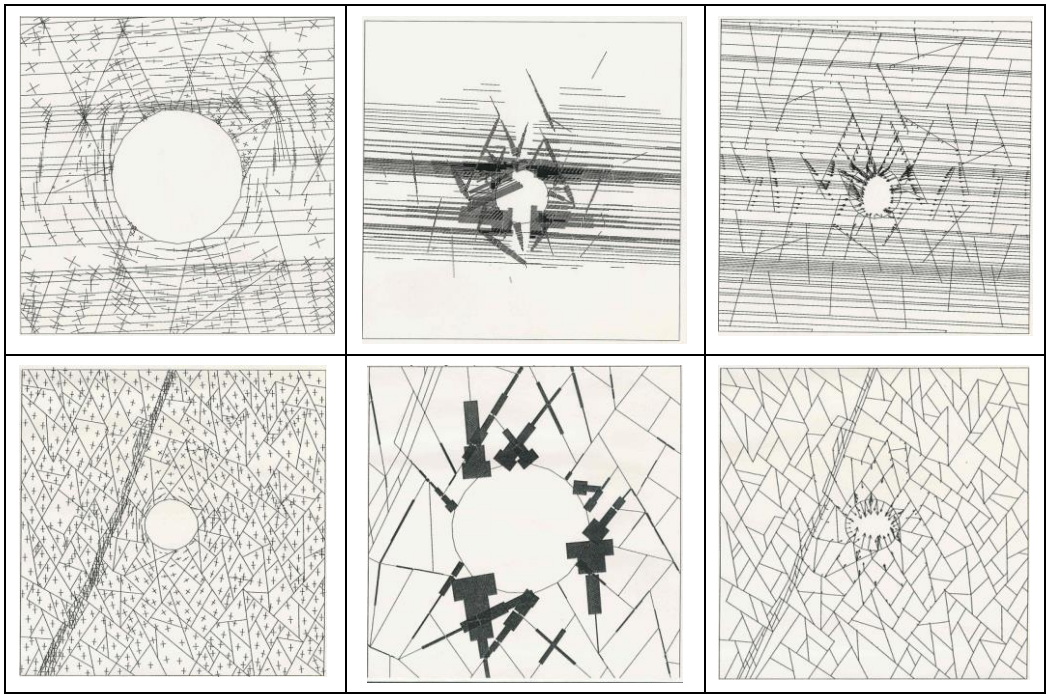

Figure 8. Selected UDEC-BB studies of a 250m deep section and a 700m deep section of a planned TBM spiral access tunnel through the interbedded St Bees sandstones and siltstones (top) and through the Borrowdale welded tuffs-ignimbrites (bottom) at the planned Sellafield LLW/ILW nuclear waste repository, from 1992. Thanks are due to NGI's numerical modelling team, during our 6 years geotechnical consultancy for UK Nirex, 1990-1996 which the author had the privilege to project-manage. All names later.

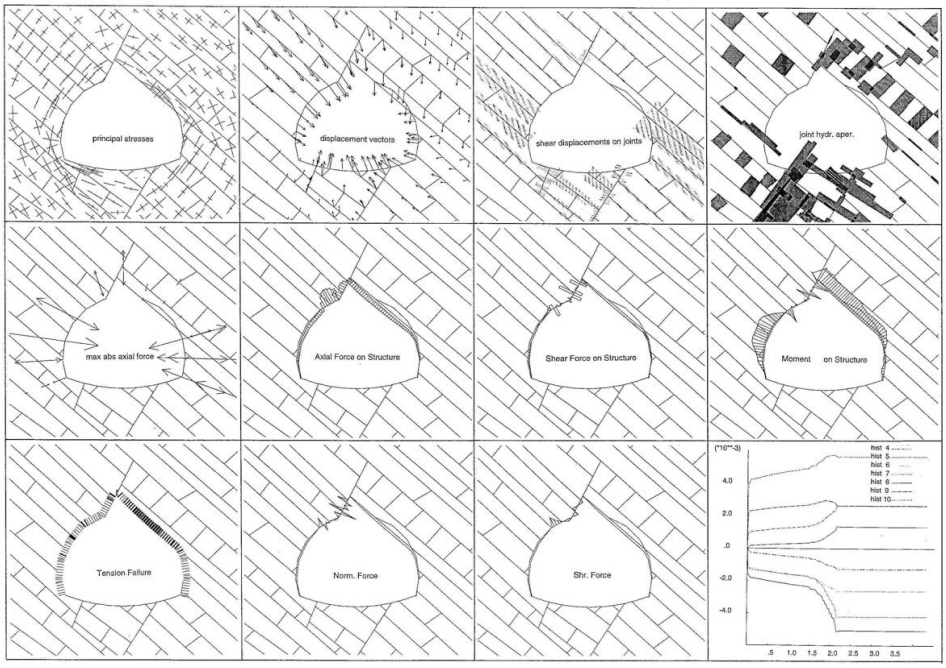

Figure 9. The discontinuum-modelling advantages of representing adversely steeply-dipping bedding. This late 1980's UDEC-BB model of a tunnel in Japan showed distinct signs of over-loading of the bolting. The bonding failure of the modelled S(fr) is also shown, bottom left.

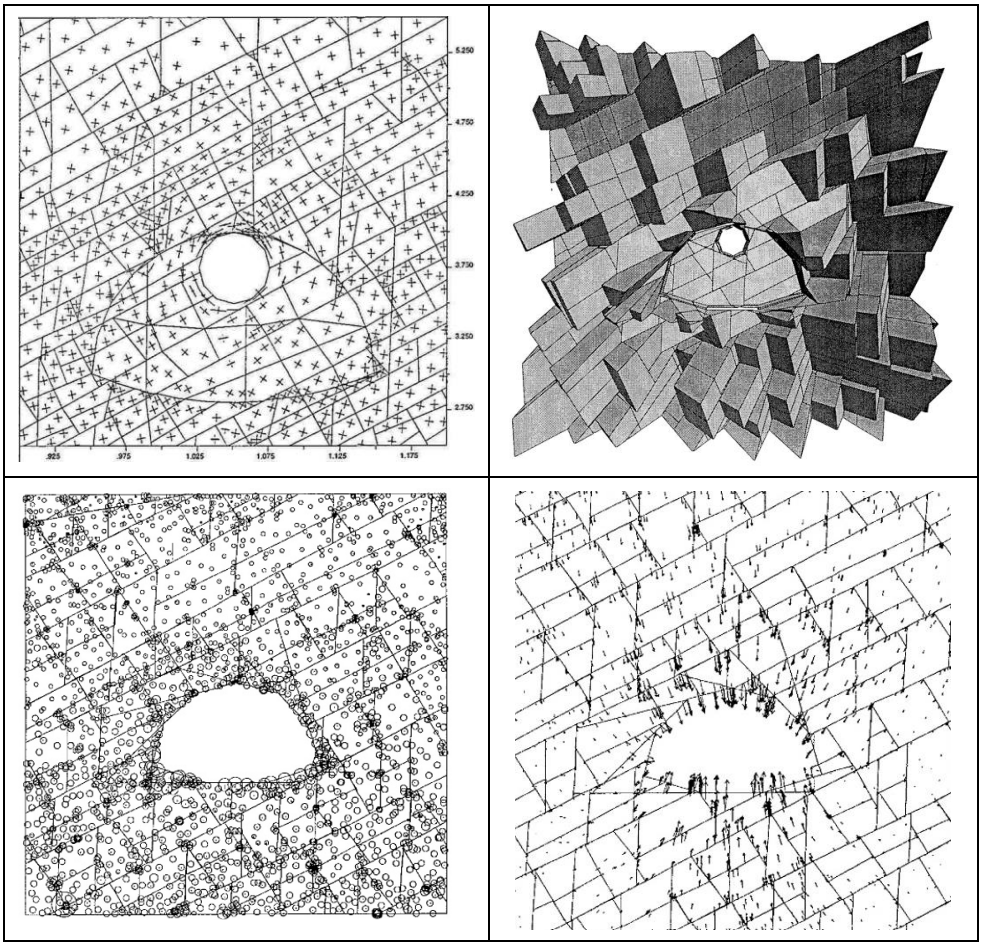

Figure 10. Top left: UDEC-BB to check TBM pilot tunnel break-out to full section. The 3DEC sections show a maximum tangential stress of 7.9 MPa and a maximum displacement of 8.0mm. This motorway project study is illustrated further in the next figure.

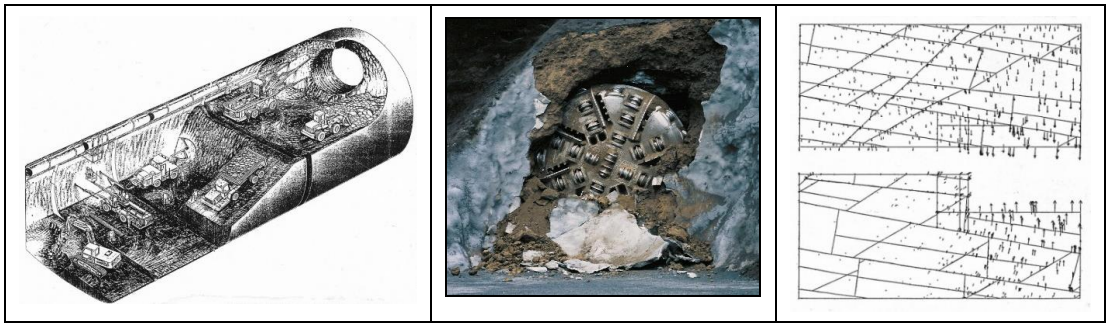

Figure 11. The unusual motorway pilot-TBM for the Tokyo-Osaka Tomei 2 Shimizu 3 motorway project. The specially designed TBM could turn so as to provide a pilot bore for the parallel tube. It proved important to 'turn' prior to reaching highly weathered rock. Dr Juhn Itoh of the Fuji Research Institute was responsible for this interesting NGI contract from Japan. NGI UDEC-BB and 3DEC modellers from the late 1980's and early 1990's included Dr Mark Christianson (Itasca/NGI) who was responsible for putting BB and UDEC 'together' in 1985 (with strong pleading to NGI's director Kaare Høeg from Barton and Bandis), Dr Axel Makurat (later Shell), Linda Hårvik, Dr Marte Gutierrez (later distinguished US professor), Dr Karstein Monsen (later Geoscan), Panos Chryssanthakis (later COWI), Dr Harald Hansteen, Dr

Baotang Shen (later CSIRO in Australia), Lise Bacher, Dr Rajinder Bhasin, Dr Lloyd Tunbridge – and since then several more.

A particularly notable discontinuum modelling contract for NGI was the design check for the designers of the 62m span Gjøvik Olympic cavern. This was done on behalf of owner Fortifikasjon, whose director Jan Rygh had drawn the 'classic serviette sketch' for the town's chief planning engineer some years earlier, before the winter games were finally awarded to nearby Lillehammer, and ice hockey was played in this unique cavern. Modelled UDEC-BB deformation 7 to 9mm, MPBX recorded deformation a constant 7 to 8mm after 5 years of monitoring.

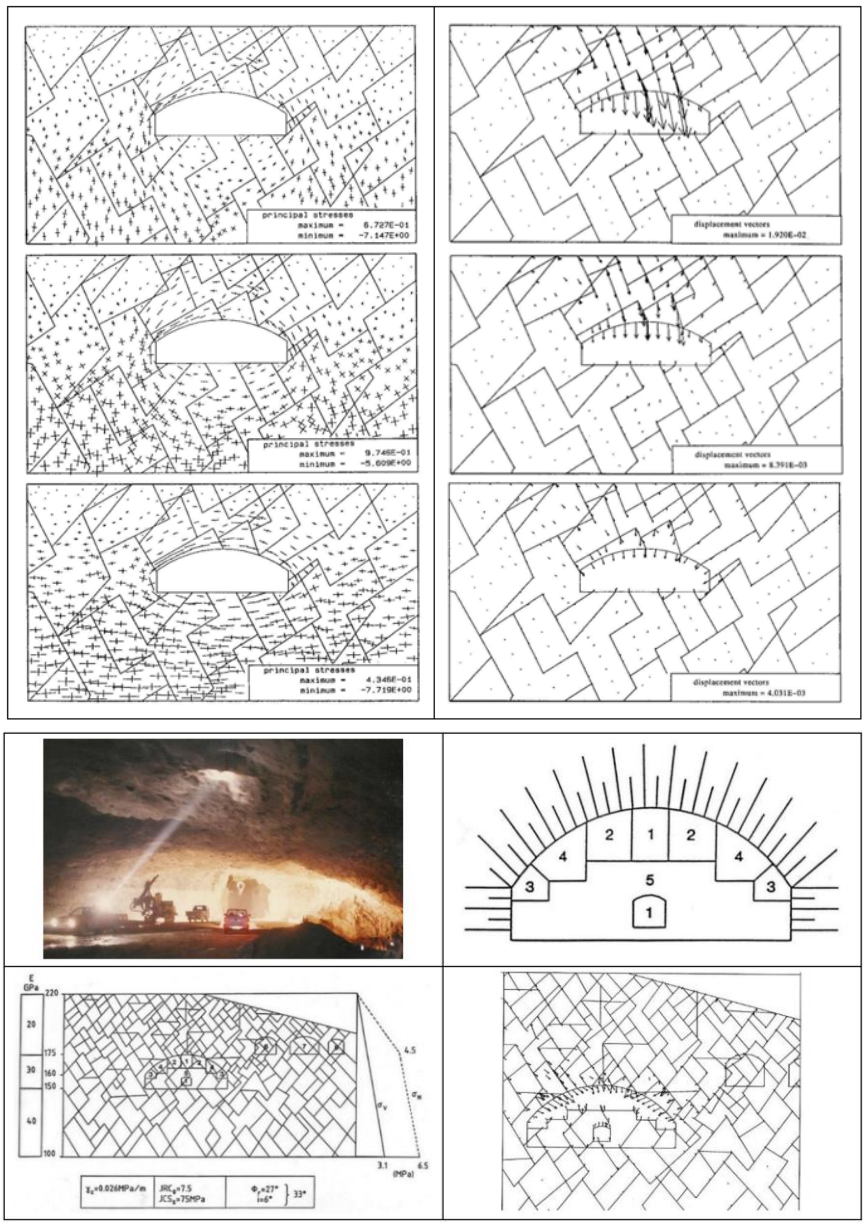

Figure 12. Top: Horizontal stress sensitivity studies conducted by Lloyd Tunbridge, and bottom: subsequently more detailed UDEC-BB modelling by Chryssanthakis, for the 62m span Gjøvik cavern. Note multi-author reference due also to Q-logging, cross-hole seismic tomography and rock stress measurement by the NGI team. Barton, Chryssanthakis, Tunbridge, Kristiansen, Løset, Bhasin, Westerdahl, Vik (1994).

4 OVERBREAK AND TUNNEL AND STOPE STABILITY

A feature of excavation effects in rock masses that particularly marks the stark difference between continuum and discontinuum modelling is *overbreak*. In Barton (2007) it was suggested that this could be quantified by the Q-parameters ratio Jn/Jr. Figure 13 (top photos and roughness sketches) shows how this works. The red- coloured ratios show Jn/Jr < 6 (no overbreak expected) while the blue-coloured ratios show Jn/Jr ≥ 6 which is the suggested criterion. Extreme-value Q-parameter statistics at the LKAB mine explain the overbreak experienced in drilling drifts. Elevated values of Ja (clay coatings) obviously add to the likelihood of overbreak.

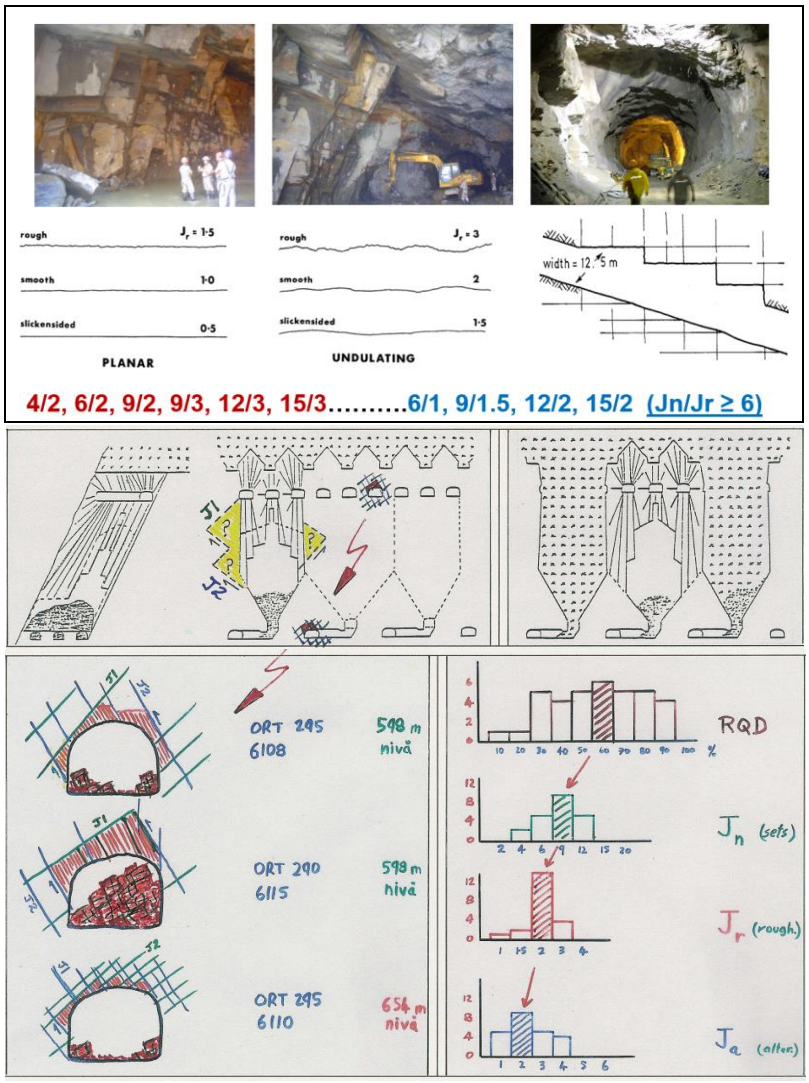

Figure 13. Top: the Q-parameter ratio Jn/Jr ≥ 6 suggests almost unavoidable overbreak if there are sufficient degrees of freedom for block fall-out (higher Jn) and if joint roughness is low enough (low Jr). Bottom: observations performed by the writer in 1988 in LKAB's 'Oscar' long-hole drilling stope-development project in Kiruna in northern Sweden. Explanations for the excessive overbreak were sought. This was the first time that *Q-parameter histograms* were used by the author, and soon this became a systematic way of logging individual Q parameters. Note the potentially serious large-scale J1/J2 deformation mechanism in the future stopes (shown in yellow). Problematic details for continuum modelers, or an interesting expansion of their possibilities to influence design decisions – in many areas.

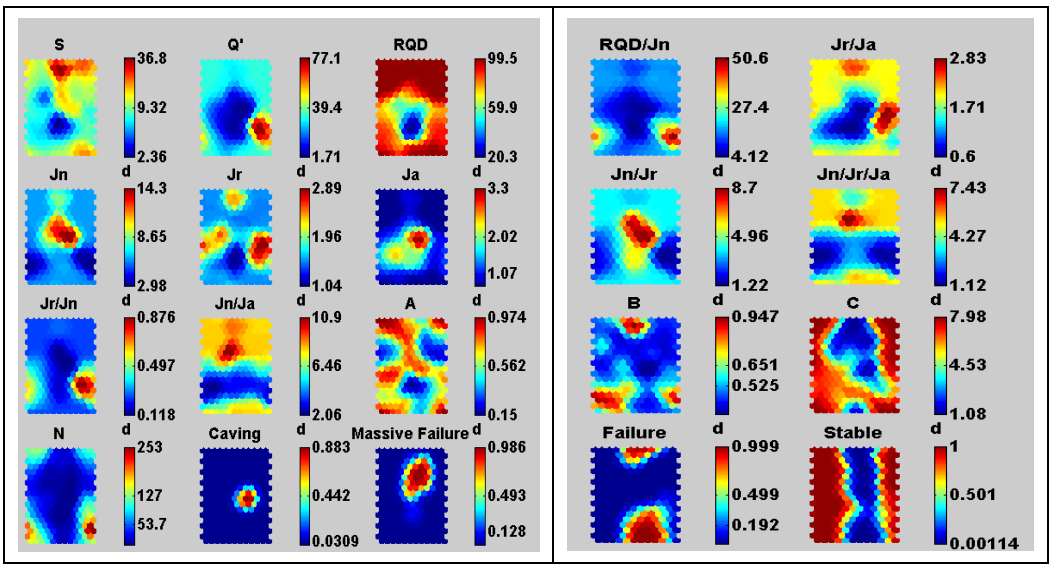

Figure 14. This 'graphical matrix' scheme developed by Dr Fraser of CSIRO, was shown to the writer during a two-days rock engineering course given in Melbourne in 2005. The subject matter is stoping for mineral extraction, and stable, caving, failure, and massive failure are the operative terms. The relative influence of various separate and combined Q-parameters are taken from the Potvin scheme of utilizing Q' = RQD/Jn x Jr/Ja in mine-stope dimensioning. 'Caving' is seen bottom-left. Jn and Ja alone, and Jn/Jr are seen to be important. They are absent in continuum modelling schemes.

5 INPUT DATA NEEDS FOR DISCONTINUUM MODELS ARE MORE THAN GSI

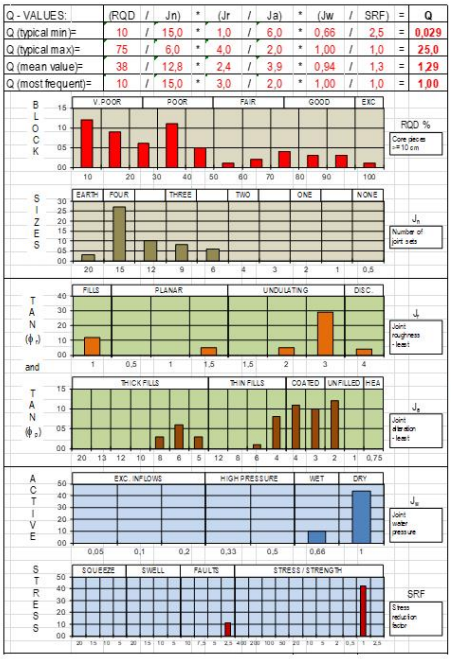

Q IS ONLY PART OF A ROCK MASS DESCRIPTION EXERCISE.

I	ROCK MASS STRUCTURE			
1	RQD	Deere et al., 1967)	block size	Q
2	J_n	= joint set number		Q
3	F	= joint frequency (per metre)		
4	J_v	= volumetric joint count (Palmström, 1982)		
5	S	= joint spacing (in metres)		
6	L	= joint length (in metres)		
7	w	= weathering grade (ISRM, 1978)		
8	α/ß	= dip/dip direction of joints (Schmidt diagram)		
II	JOINT CHARACTER			
9	J_r	= joint roughness number	shear strength	Q
10	J_a	= joint alteration number		Q
11	JRC	= joint roughness coefficient		
12	a/L	= roughness amplitude of asperities per unit length (mm/m)		
13	JCS	= joint wall compressive strength		
14	ϕ_r	= residual friction angle		
15	r,R	= Schmidt rebound values for joint and rock surfaces		
III	WATER, STRESS, STRENGTH			
16	J_w	= joint water reduction factor	active stress	Q
17	SRF	= stress reduction factor		Q
18	K	= rock mass permeability (m/s)		
19	σ_c	= compressive strength		
20	σ_1	= major principal stress		

Figure 15. The six Q-parameters (seen as histograms on the left) that are used in characterizing rock masses and tunnelling conditions more fully are obviously just part of the comprehensive data needed for a thorough engineering geological description. Serious consultants do not / should not put a 'blob' on a GSI chart and be satisfied that it will give the required input data for their ('black-box') modelling.

Three of the most commonly used shear strength criteria for rock joints are illustrated in Figure 16. The classic Mohr-Coulomb involving a cohesion intercept 'c' and a stress-independent friction angle 'φ' *was not developed from testing rock joints*, which actually do not display actual cohesion intercepts unless very steep (60-90º) steps are present in the joint plane, due for instance to cross-joint influence. An improvement for lower stress was suggested by Patton, 1966 with his well-known 'i-values' where 'φ + i' will be the lower-stress estimate. The problem of course is which combination of 'i-values' one should use. This was the impetus for a new student in 1966, and the resulting parameters described below took some years to materialize.

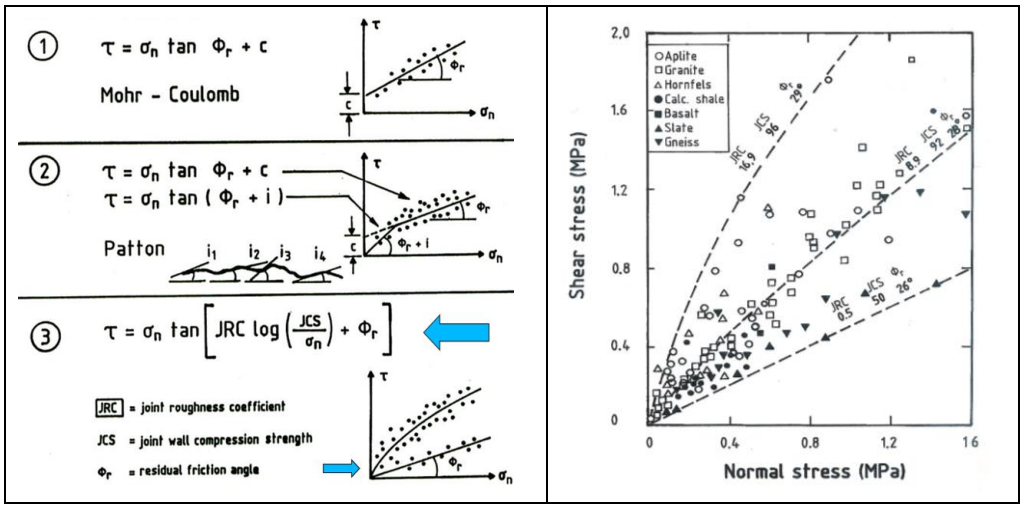

Figure 16. Mohr-Coulomb, Patton (1966) and Barton (1973) shear strength criteria for rock joints. The first version of the JRC, JCS, φ_r criterion (in 1967) was developed from DST tests on 200 tension fractures. One is shown in Figure 2: with respective values of 20, UCS (since no weathering) and 30º.

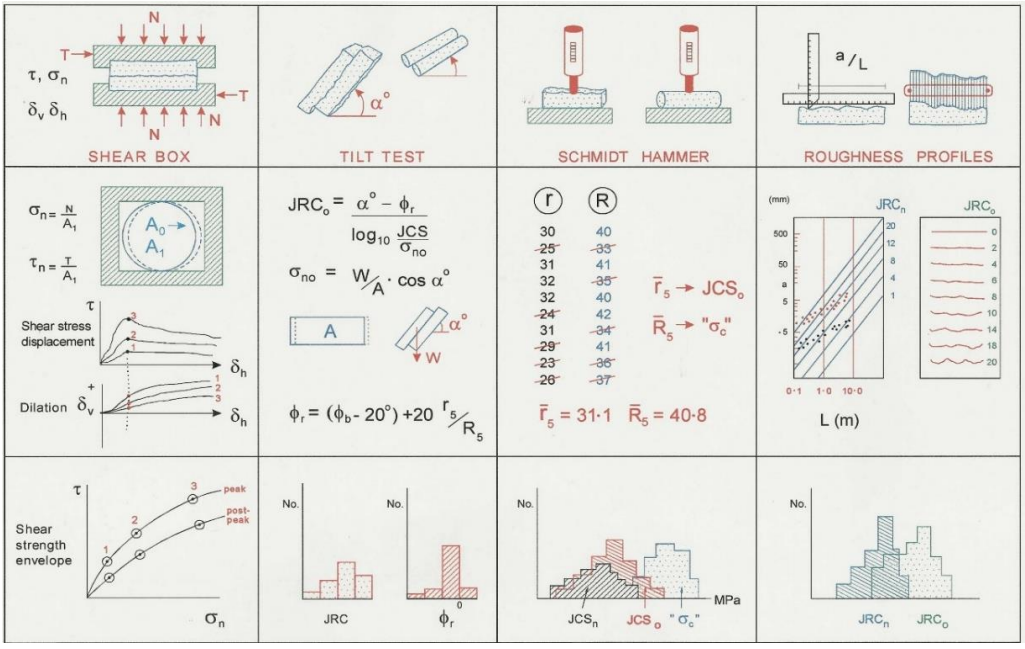

Figure 17. Shear box, tilt test, Schmidt hammer and roughness profiling methods (including a/L) used for evaluating the JRC, JCS and φ_r data for UDEC-BB and other discontinuum modelling projects.

In the case of NGI's Sellafield project for UK Nirex (1990-1996) some 10 kilometers of core were logged and numerous joint samples representing each joint set were prepared. Besides tunnel models (Figure 8) a large number of deep cavern models in welded tuff (ignimbrite) were also performed using UDEC-BB to check on self-supporting abilities and EDZ depths. Note that multi-stage shear testing of the same joint sample at increasing normal stress causes rotation of the shear strength envelope. (Barton, 2013). This gives artificial 'life support' for 'c' and also gives reduced 'φ'. (Increased open pit costs if 'c' is ignored and set to 'zero' with 'φ' too low).

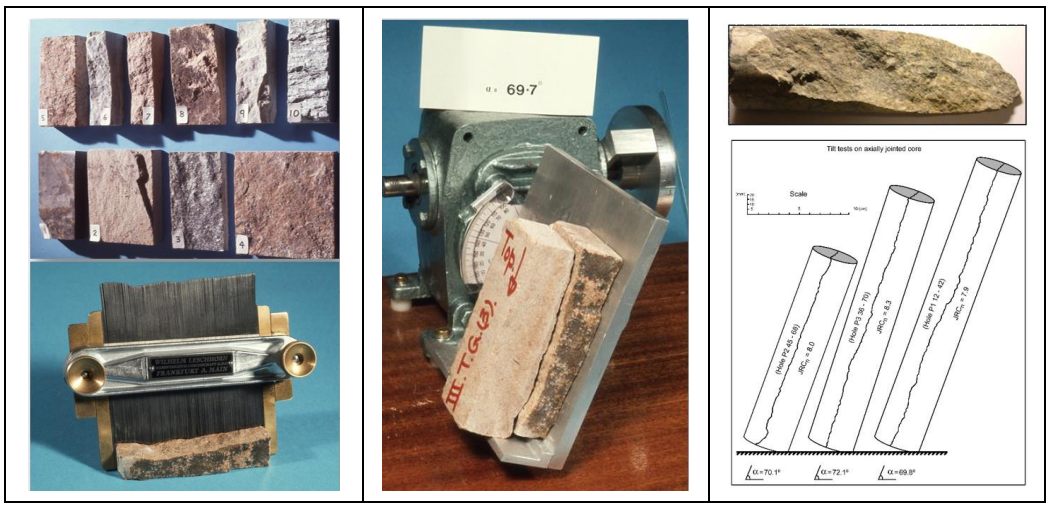

Figure 18. Left: examples of joint profiling and tilt tests. From Barton and Choubey (1977). Note that the profile gage had four 'shims' per millimeter. There were no steps as some critics have assumed. Right: tilt-tested joint samples (at correct angles) from TerraTek's heated block test in Colorado. Barton, 1982.

6 WHEN CONTINUUM MODELLING CAN BE THE ONLY CHOICE

A suggested scheme for choosing *which type* of computer modelling is appropriate for *which type* of rock mass, is shown in Figure 19. In the earlier examples of UDEC-BB given in this paper, we were well within the suggested Q-range of 0.1 (very poor) to 100 (very good). It was possible for engineering geologists (in the case of the UK Nirex project it was often Fredrik Løset) to suggest a realistic and representative joint pattern, which was digitized so that it could be reproduced as perhaps one of several UDEC model geometries. One can 'move models around' in a big jointing 'template' and include faults in some models.

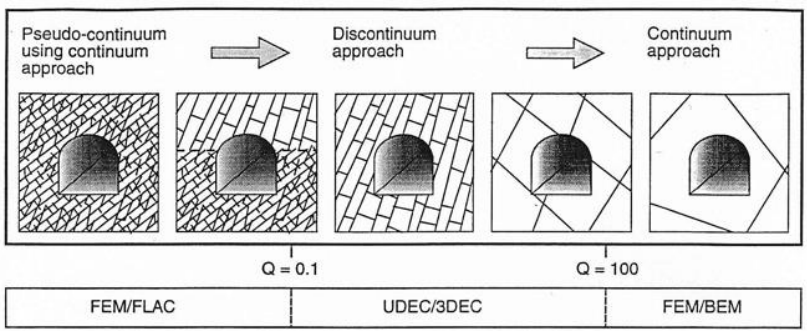

Figure 19. A scheme for helping in the selection of appropriate computer models, based on a 'degree-of-fracturing' scheme with suggested Q-value scale for UDEC and 3DEC. Continuum at either end implied.

If the rock mass is highly fractured as symbolized in the left side of Figure 19, then a continuum approach may be needed. Logic would suggest that Q is stretched to 0.01 or worse to the left side, and to an almost unjointed Q = 500 to 1000 on the right side. However, care is needed in assuming that GSI and Hoek-Brown equations of assumed rock mass behaviour will give relevant results. There is unfortunately evidence of grossly exaggerated 'plastic zone' prediction, as revealed in an international court case some years ago. This can hardly be due to the commercial FEM method used at that time though it might be partly due to *adding* the strength components related with 'c' and 'φ'. ($c + \sigma_n' \tan \varphi$).

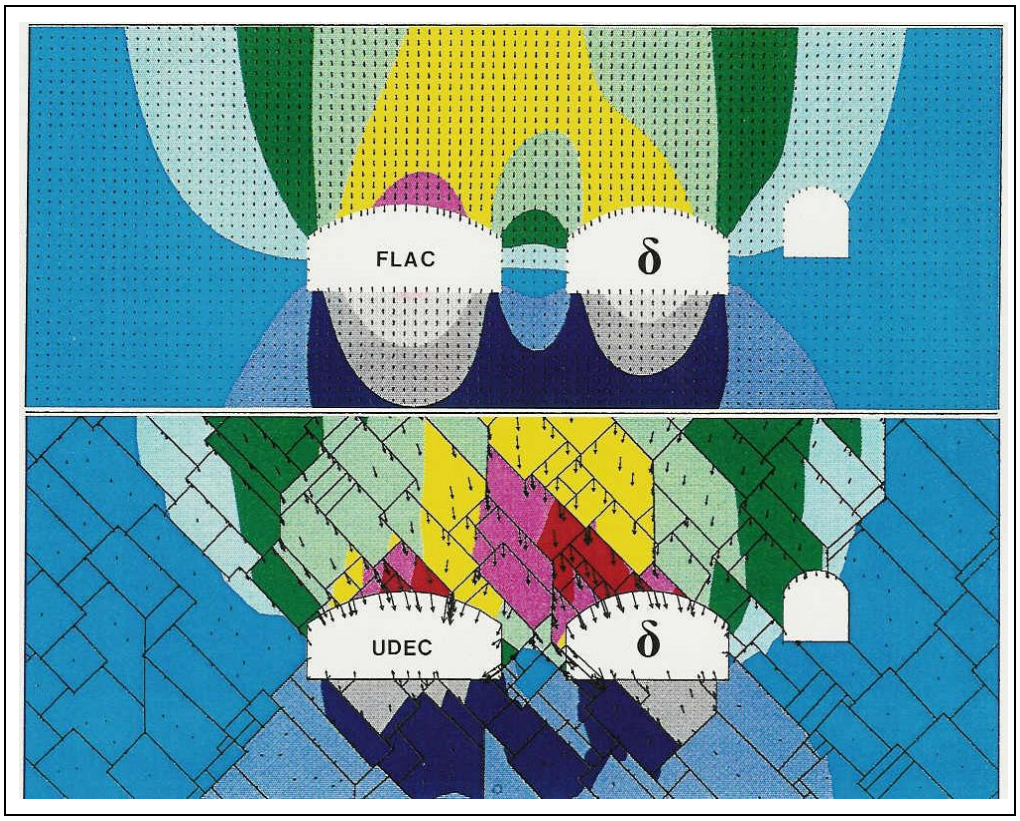

Figure 20. Comparison of FLAC and UDEC-BB by a former NGI colleague Lise Backer (now BaneNor). The same triple-tunnel motorway is modelled using the same boundary stresses and the same intact-block moduli. The jointing makes the UDEC-BB model significantly more relevant than the continuum model. Anisotropy and pillar distress is also seen.

In Figure 20 a continuum model using FLAC is compared with a UDEC-BB model. In this particular case low Q-values are not being modelled, so the deformation is small in both cases, but the UDEC-BB model teaches us much more than the continuum FLAC model.

In the next figure we see something that was a great surprise to the present author when first seen in an SKB document with Prof Derek Martin as lead author. The date was 2002 or 2003. Figure 21 shows part of the PhD study by an Iranian author: Dr. Hajiabdolmajid. In his 2000 publication he is supported by his presumed internal and external supervisors Prof Derek Martin and Dr Peter Kaiser, both well known specialists in rock engineering and mining engineering. The results they present, reproduced in Figures 21 and 22 were very important, but a huge majority of people working in rock mechanics have ignored the message and continue with GSI, Hoek-Brown equations and FEM continuum software with '$c + \sigma_n \tan \varphi$'.

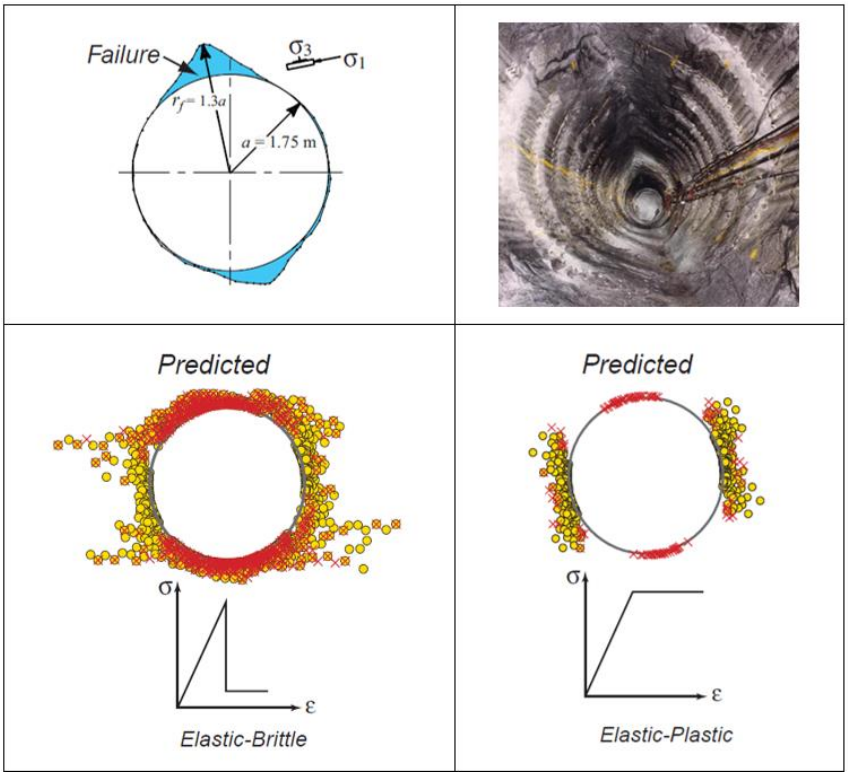

Figure 21. Mohr-Coulomb tri- and bi-linear elastic-brittle and elastic-plastic models of the well-known URL (Manitoba) line-drilled mine-by tunnel. Magnitudes of the input parameters came from GSI and H-B estimation. The objective of the modelling was to show the great improvement that results if the cohesion is degraded while friction is mobilized, shown in Figure 22. The Mohr-Coulomb results are surprisingly unrealistic, yet the criterion is so widely used. It is remarkable that so much incorrect modelling is performed. The three authors are listed here Hajiabdolmajid, Martin and Kaiser (2000).

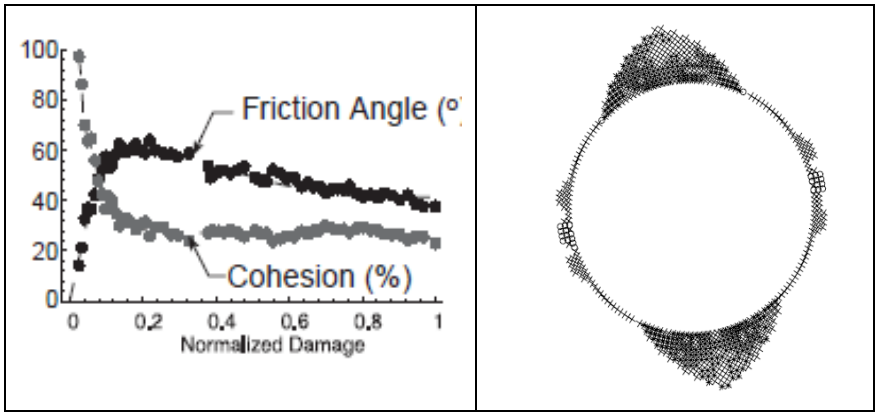

Figure 22. A greatly improved result using a CWFH (cohesion weakening friction hardening) approach. Hajiabdolmajid et al. (2000). The over-stressed volumes do not fall out as the analysis is still a continuum solution, but the reality of location is convincing. The author and a colleague (Barton and Pandey, 2011) also used this CWFH approach in mine stope modelling using Q-based input data CC and FC (see Barton, 2002) in FLAC3D models of pre-instrumented stope areas.

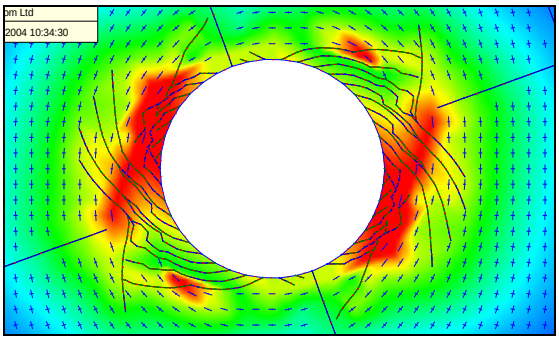

Figure 23. The BEM fracture mechanics code FRACOD developed by Shen et al. (2013). This shows a realistic development of log-spiral failure surfaces when jointing is sparse (the right-hand side of Figure 19). Red represents low, and green represents high factor of safety against further fracturing. In situ stress levels were > 40% of UCS. These were scoping studies for the sub-Andean Olmos tunnel where there were rock-burst challenges, since a 'stress-raising' TBM had to be used in the new contract. Shen 2004.

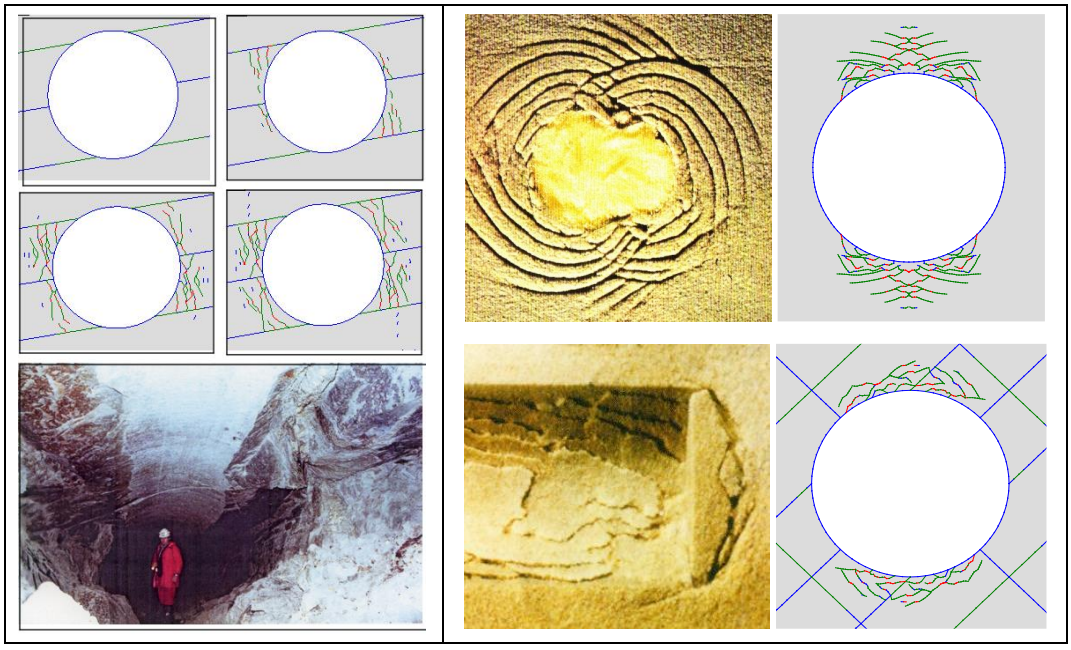

Figure 24. Left: FRACOD BEM fracture mechanics model of failure in a TBM tunnel (the English/Old Beaumont tunnel). Centre: physical model of a bored tunnel (or well) in a 3D loaded block showing intersecting log-spiral shear surfaces due to inclined boring. Right: FRACOD models of 1,000m deep TBM tunnel in massive or jointed rock. Shen and Barton, 2018. This 'starting as a continuum' model (FRACOD) is of course in an elevated category in relation to the usual 'continuously' continuum models.

7 A CRITIQUE OF GSI, HOEK-BROWN EQUATIONS, AND THEREFORE CONTINUUM ANALYSES THAT DEPEND ON THEM

In the opinion of the author it is rather remarkable and somewhat discouraging for the past and future of our subject 'rock engineering', that so many young (and not so young) people have adopted the RocScience-promoted and of course Hoek-promoted GSI, with the associated Hoek-Brown equations. The following three pages (by others) came as a shock to this author.

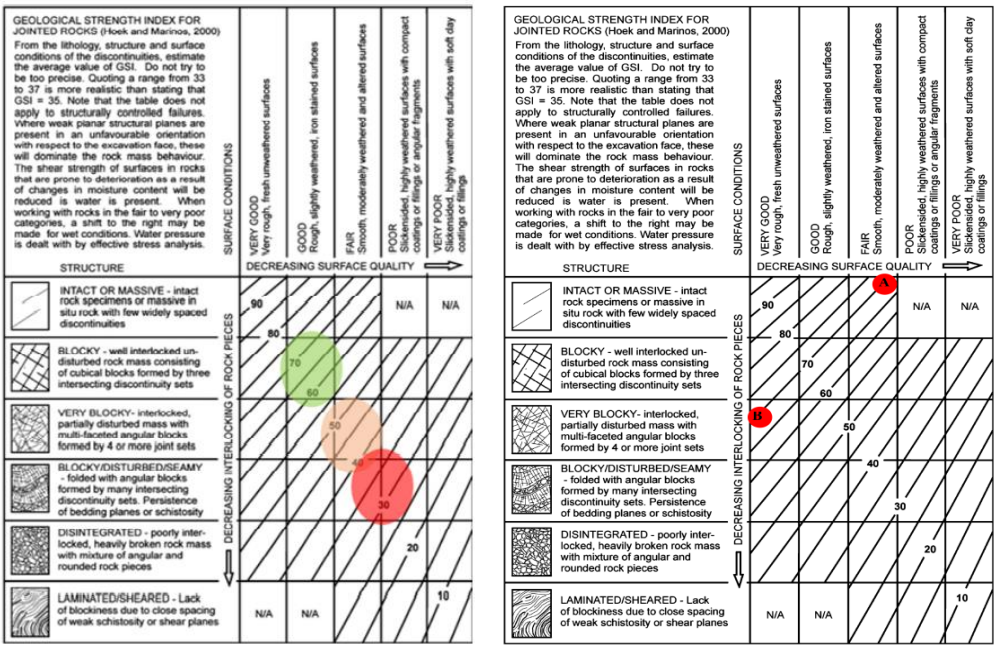

$$C_m = \frac{\sigma_{ci}\left((1+2a)s + (1-a)m_b\sigma_{3n}\right)\left(s + m_b\sigma_{3n}\right)^{a-1}}{(1+a)(2+a)\sqrt{1 + \left(6am_b\left(s + m_b\sigma_{3n}\right)^{a-1}\right)/(1+a)(2+a)}}, \quad (1)$$

$$\phi_m = \sin^{-1}\frac{6am_b\left(m_b\sigma_{3n} + s\right)^{a-1}}{2(1+a)(2+a) + 6am_b\left(m_b\sigma_{3n} + s\right)^{a-1}}, \quad (2)$$

$$\sigma_{3n} = \frac{0.47\sigma_{cm}^{0.06}(\gamma H)^{0.94}}{\sigma_{ci}}, \quad (3)$$

$$m_b = m_i \exp\frac{\mathrm{GSI} - 100}{28 - 14\ D}, \quad (4)$$

$$\sigma_{cm} = \sigma_{ci} \cdot \frac{\left(m_b + 4s - a\left(m_b - 8s\right)\right)\left(m_b/4 + s\right)^{a-1}}{2(1+a)(2+a)}, \quad (5)$$

$$E_{rm}(MPa) = 100.000\ \frac{1 - D/2}{1 + e^{(75+25D-GSI)/11}} \quad (6)$$

$$E_{rm}(MPa) = E_i\left(0.02 + \frac{1 - D/2}{1 + e^{(60+15D-GSI)/11}}\right) \quad (7)$$

Figure 25. The GSI-rating selection scheme based on a brief encounter with ‘geology’ (the sketches) is followed by what could truly be called black-box modelling. Where does the number of joint sets actually appear? Why does slickensiding have to be ‘highly weathered? Why cannot rougher joints have clay filling and be weathered? GSI is actually the least logical and least ‘geological’ method in use in rock engineering, and the sequence of Hoek-Brown equations are much more a priori than a posteriori (Barton, 2011). Yet one researcher recently expressed the opinion that finally one has a ‘geological’ classification method. The reality is that any chance of ‘geology’ is immediately smoothed in a ‘continuum blender’ giving different viscosities i.e. shear strength. The result is not a geological representation of rock masses. (Hoek et al. 2002, Renani & Cai, 2021).

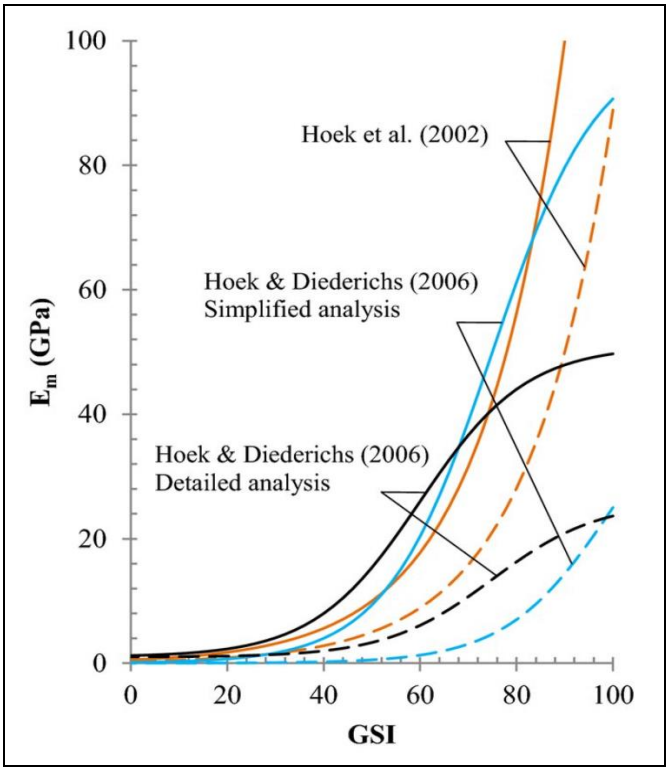

Figure 26. The widely varying deformation modulus estimates connected with GSI. From: Renani & Cai (2021): Forty-Year Review of the Hoek–Brown Failure Criterion for Jointed Rock Masses. One may seriously ask how continuum modellers are choosing deformation modulus. Perhaps by waiting for the results of the modelling and adjusting the disturbance factor D? Several private communications have stated such, and if this is so it seems hardly defensible for presenting to a client.

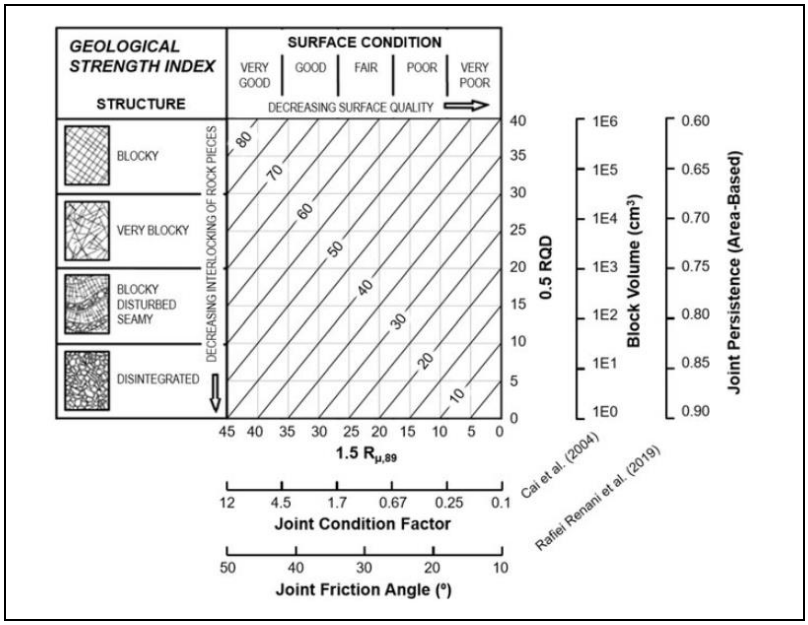

Figure 27. Surprisingly creative additions for 'better' quantifying GSI. Renani and Cai, 2021. The better-known methods are listed in Table 1. It is a somewhat surprising list. With all the proposed improvements what happens to the predicted H-B shear strength results? Is this a form of empiricism or just guessing?

Table 1. A selection of some equations used to improve the quantification of GSI. Why a published and widely used method should require so much improvement, or indeed be used by so many with such apparent confidence, is not clear. Ván & Vásárhelyi (2014).

$GSI1 = RMR - 5 = R1+R2+R3+R4+R5(=15) - 5$	(1)
$GSI2 = 1.5\ R4 + 0.5\ RQD$	(2)
$GSI_3 = 15 \log\left(\frac{RQD}{Jn}\frac{Jr}{Ja}\right) + 50$	(3)
$GSI_4 = 9 \ln\left(\frac{RQD}{Jn}\frac{Jr}{Ja}\right) + 44$	(4)
$GSI_5 = \frac{52Jr/Ja}{(1+Jr/Ja)} + 0{,}5RQD$	(5)
$GSI_6 = \frac{26{,}5 + 8{,}79\ln Jc + 0{,}9\ln Vb}{1 + 0{,}0151\ln Jc - 0{,}0253\ln Vb}$	(6)
$GSI_7 = 153 - \frac{165}{\left[1+\left(\frac{Jp}{0{,}19}\right)^{0{,}44}\right]}$	(7)

8 EXAMPLES OF ROCK SLOPES: REAL, DISCONTINUUM, CONTINUUM

With the exception of highly trafficked road-cuttings and railway-cuttings, and steep urban slopes above busy pavements, there will generally not be much enthusiasm for bolting or cable anchors for ensuring rock slope stability in general. This is because there are millions and millions of rock cuttings and they cover a huge area all around the world. Of course, this support reluctance will not apply to some critical high-dam valley slopes as especially seen in deep and already naturally over-steepened valleys in China,

Temporary and more permanent open-pit mine slopes suffer the same no-bolting fate for obvious economic reasons. Since there may be no rock bolts, the alternative selection of *stable slope angles* will usually have to depend on the shear strength properties of the local rock joints, and especially joint orientations. This is the philosophy behind Q_{slope}. The first client wanted a 20km dam access road in a steep valley without bolts. (Barton and Bar, 2015). Some five hundred design-chart case records mostly collected by Bar are shown later. (Bar and Barton, 2017).

Of more concern in this final section is the misinformation promoted by commercial software companies, who hold courses showing the popular but hardly existing curved ('spoon-shaped') potential failure surfaces that are relevant for soil slopes and rockfill, *but not for slopes in jointed rock* unless this is extremely weak. (In fact, in about 1968 the author had sketched a curved failure surface for completely disintegrated slates in an open pit, but such weakness is the exception as most of our civil and mining slopes are in jointed rock with enough strength to cause deformation along discontinuities as opposed to ignoring their existence.) It seems that the assumed 'rock mechanics' modelling performed by hundreds or perhaps thousands of young engineers has actually been based on old-fashioned soil mechanics continuum principles, and such is regrettably the case when adding c and σ_n tan φ as in misleading Mohr-Coulomb and Hoek-Brown methods. Figure 28 shows some alternatives that address discontinuities, whether joints or filled discontinuities or fault planes., from Hoek and Bray (1974) and Barton (1971).

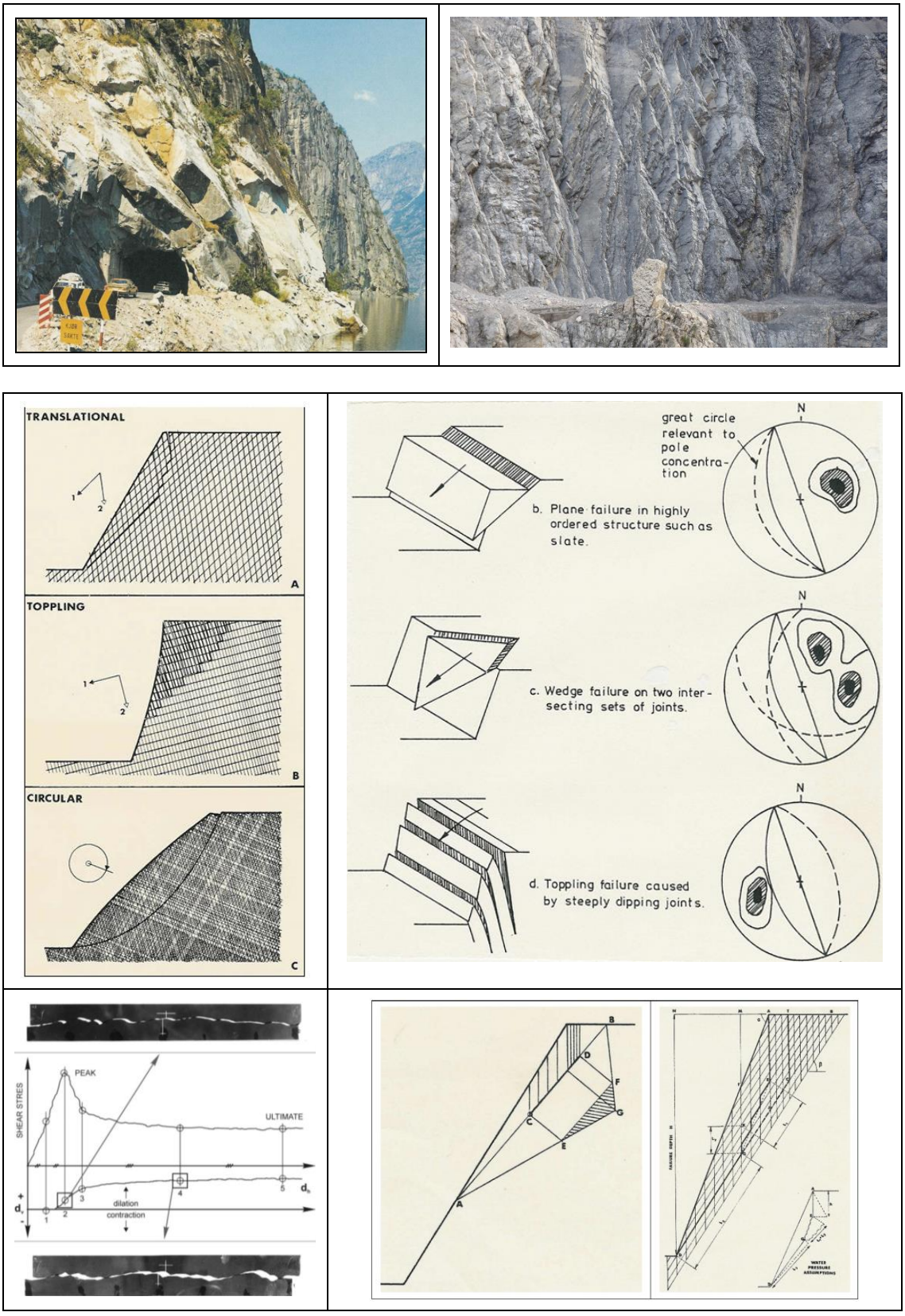

Figure 28. Reality and representation – as discontinua. Central right diagram: Hoek and Bray.

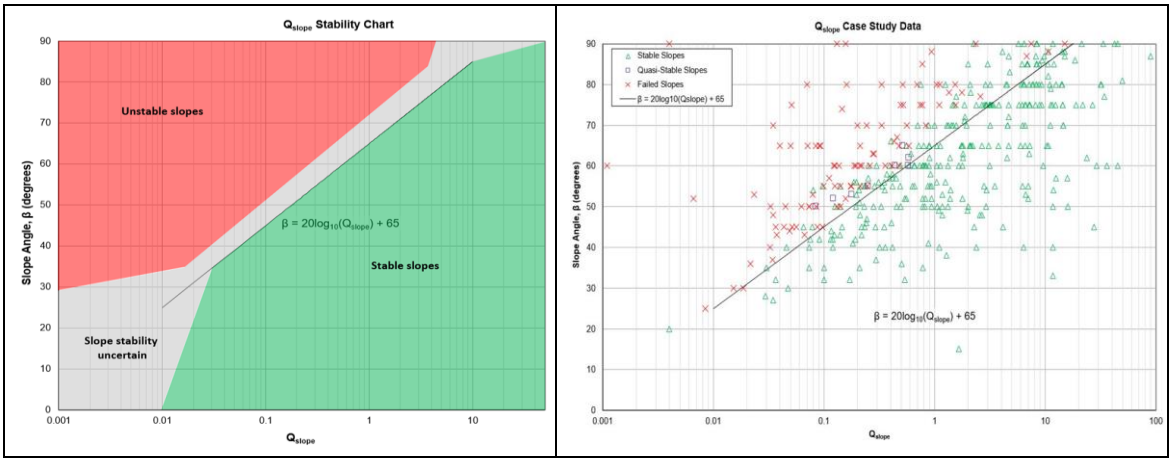

Figure 29. The Q_{slope} method is based on Q parameters with almost unchanged RQD, Jn, Jr and Ja. However wedge stability is considered so pairs of Jr/Ja apply to different sides of potential wedges, with relevant orientation weightings. Since slopes are under lower stress than many tunnels, SRF has three appropriate categories, and Jw is now called J_{wice}. The relative effects of tropical rain and ice-wedging can be roughly assessed. Co-author Neil Bar has been a very active collector of case records. Barton & Bar (2015), Bar & Barton (2017). Q_{slope} : 0.01, 0.1, 1, 10, 100. Critical slopes: 25°, 45°, 65°, 85°, 'half tunnels' meaning over-hang is possible. Not advised but likely to be possible due to cohesive strength.

Returning to continuum models, according to Styles & Vakili (2020), the recently developed *Improved Unified Constitutive Model* (IUCM) 'takes the best parts of Mohr-Coulomb and Hoek-Brown, with integrated confinement-controlled softening/hardening of cohesion and friction, confinement-controlled changes in the dilation angle, and porosity-controlled modulus softening'. However, the slope failure predictions shown in Figure 30 represent something usually only seen in rockfill or hard soil. The 'spoon' mode shown apparently has a limited actual relation to geology or jointed/faulted rock. Open pit slopes fortunately seldom if ever fail like this.

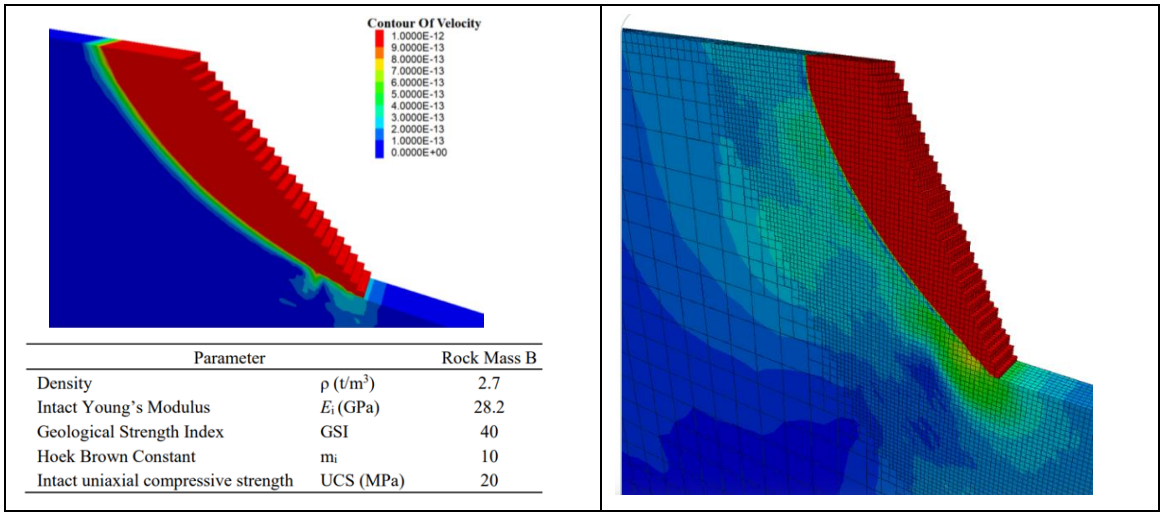

Parameter		Rock Mass B
Density	ρ (t/m^3)	2.7
Intact Young's Modulus	E_i (GPa)	28.2
Geological Strength Index	GSI	40
Hoek Brown Constant	m_i	10
Intact uniaxial compressive strength	UCS (MPa)	20

Figure 30. FLAC3D slice of a 200m high open-pit slope, using the IUCM constitutive model. Such spoon-shaped failure is possible in rockfill and in hard soil, but the writer does not believe it has been seen in competent jointed and sometimes faulted rock. Perhaps with this relatively low UCS = 20MPa input, such an unusual (for rock) failure mode is possible. Styles & Vakili (2020).

The circular failure beliefs of Mohr-Coulomb and Hoek-Brown modelers, with Carranza-Torres (2021) a presumed chief contributor and probably largely responsible for the smooth curves of the H-B rockmass criterion of Hoek et al. (2002) and the associated most complex equations, has given a very detailed recent treatise concerning 'rock slope' stability. Figure 31 is his clear but apparently misleading introduction, as it does not and cannot correspond to slope failure in competent, jointed, and perhaps faulted rock because the UCS and actual cohesion are too high in relation to the artificial 'lowering' in the H-B shear strength beliefs.

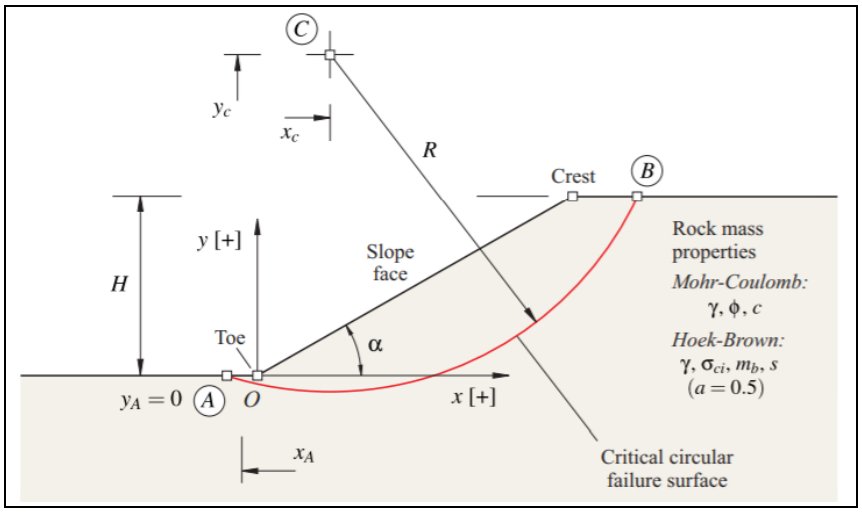

Figure 31 According to Carranza-Torres, 2021 this figure represents 'a section of a rock slope in a rock mass that obeys the Mohr-Coulomb or Hoek-Brown failure criteria'. Slopes in competent jointed rock cannot actually fail as in this figure. A continuum myth is presented, only valid for very weak saprolite or soil-like material.

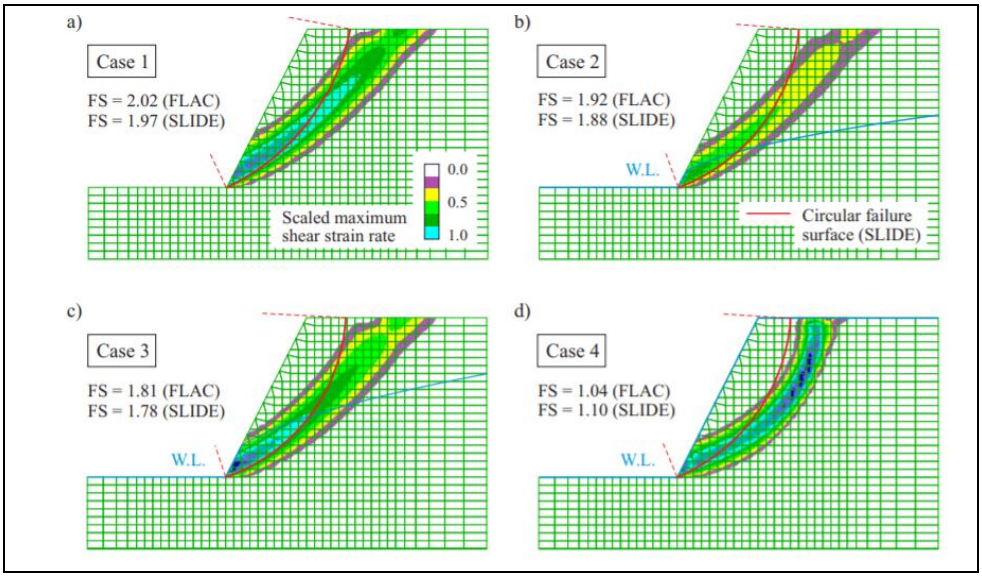

Figure 32. Further 'circular' failure analyses using both FLAC and SLIDE computer modelling, apparently with input of c and φ derived from combined GSI and Hoek-Brown. Carranza-Torres (2021). These are basically resembling failure in hard soil, perhaps also very weak rock like saprolite, and rockfill.

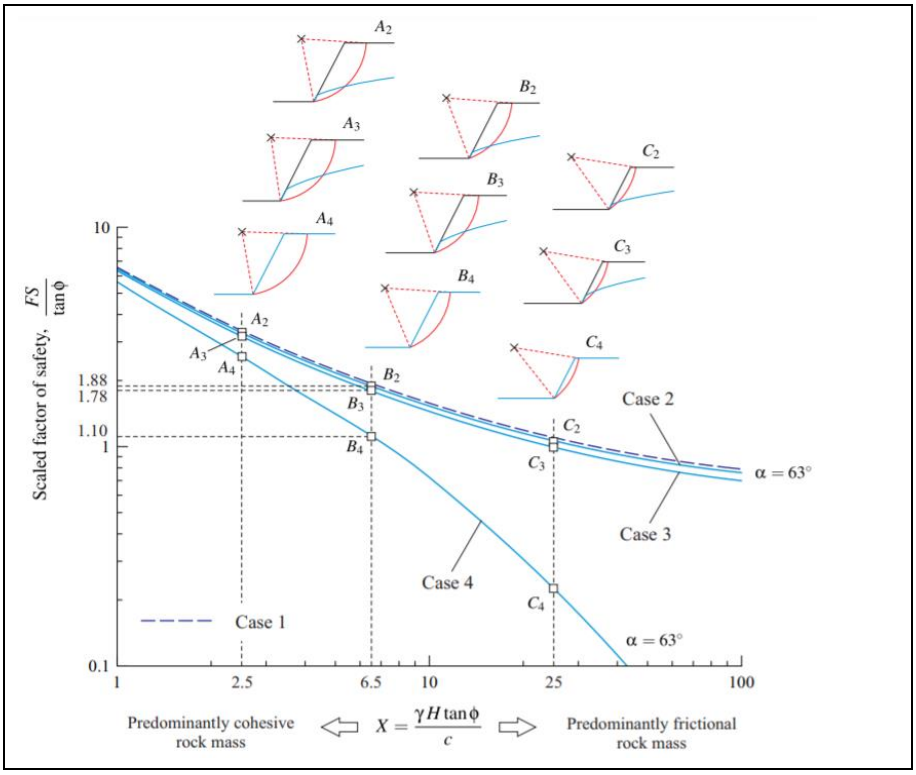

Figure 33 The 'elegance' of the relative 'c' or 'φ' dominance given by Carranza-Torres (2021) in his many impressive 'design charts' cannot be denied. The relative depths of the various spoon-shaped predicted failures are interesting. But they do not apply to competent jointed rock. Joints sets, intact bridges, and possible faults are each going to bring back reality.

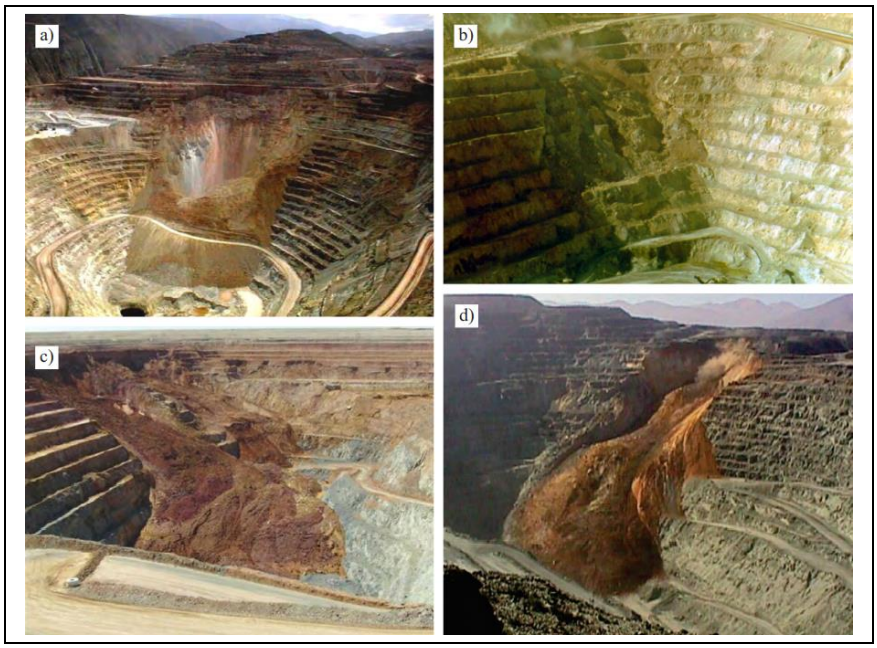

Figure 34. Four major open-pit failures reproduced by Carranza-Torres (2021).

The four major open-pit failures shown in Figure 34 were reproduced again by the present author, but for different reasons compared to Carranza-Torres. Cases a) and b) are strictly 'internal' failures that hardly extend to the crest of the slopes. Only case b) looks like jointed rock. Case c) is lake-bed sediments and saprolite, so not jointed rock. Case d) which certainly extends beyond the pit crest is actually an example of a wedge failure (Lorig et al. 2009), as was also the case for the record Bingham Canyon mine failure shown in Figure 35.

Case d) was a major slope failure in northern Chile. Looking closer to the source, Chapter 10 of the invaluable 'Guidelines for Open Pit Slope Design edited and partly written by John Read and Peter Stacey, we can see reference to the failure as a 'wedge failure' example (Lorig, Stacey and Read, Chapter 10: their Figure 10.12 caption reads: 'Wedge failure disrupting the entire slope'. So it is not an example of 'circular' (or 'spoon-shaped') failure. An even larger (and world-record) failure involving a major planar discontinuity is shown in Figure 35.

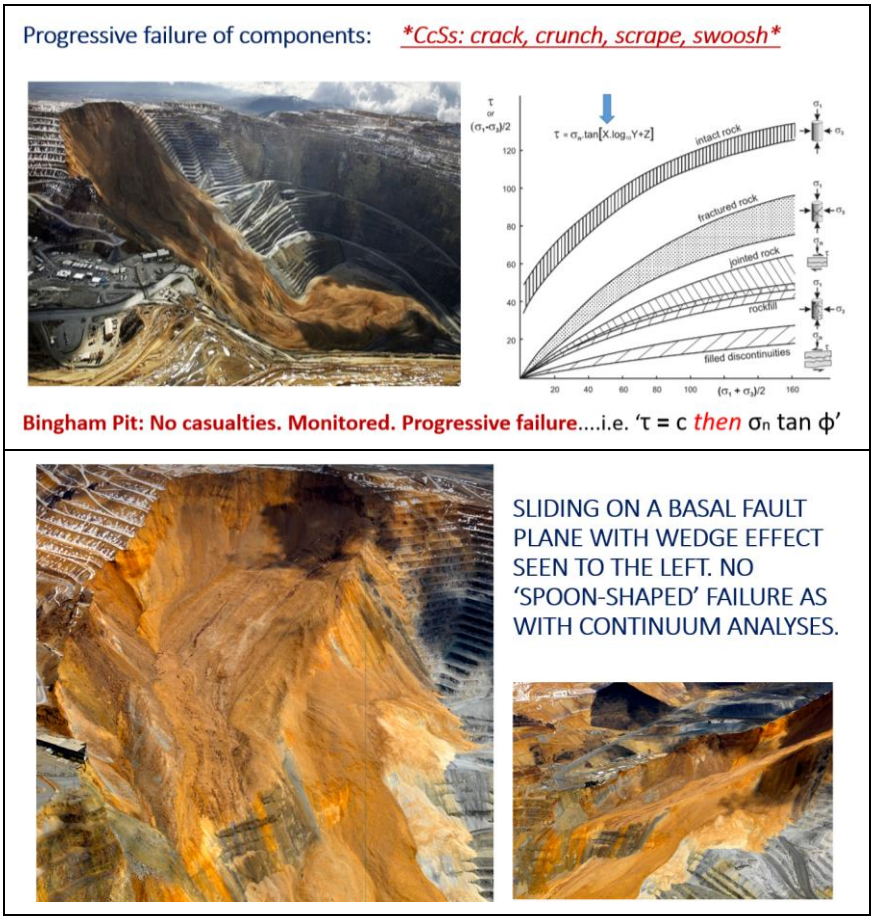

Figure 35 Bingham Canyon mine with its 70,000,000 m^3 failure. From top-to-toe the slide measured a surprising 3km, and the debris looks like a frozen 'liquid'. The adverse (tangential stress eliminating) 'nose' and a major discontinuity (a fault?) of many 100's of meters length seem to be the main culprits.

9 CONCLUSIONS

1. In this lecture the writer has suggested 'putting back jointing and geology' into the practice of rock mechanics modelling and understanding. Following the limitations but useful lessons from physical fracture models, a number of UDEC-BB models were re-

produced to emphasize the possibility of representing some details of 'geology and structure' at least in 2D and occasionally in the more demanding 3DEC.

2. GSI with the 'G' in its initials has actually removed the geology from our subject, once users leave the six 'sketches' and progress to the Hoek-Brown equations and commercial software with the impressive but misleading curves of shear strength. Regrettably the uniquely opaque 'black-box' analyses effectively become homogenized as in a food blender, but with variable viscosities. Continuum behaviour is clearly misleading many and, in the opinion of this author, is hardly to be considered as rock engineering or rock mechanics since missing engineering geology input. Looking at sketches and guessing a representative 'joint condition' (and modulus) is not defensible.
3. We have been warned for more than 5 decades – historians in our subject would claim even longer – that we should not add 'c' and the frictional component of strength based on 'φ' ($\sigma_n \tan \varphi$). At the very least it should be *'c then sigma n tan phi'.* This separation in time and deformation is logical and urgently needed.
4. A newer proposal for a more comprehensive (progressive) failure criterion is the CcSs *'crack' 'crunch' 'scrape' 'swoosh'* concept applied in Barton (2021). This has the ability to add the progressive contributions of the broken cohesion of rock bridges, the resulting rough, fresh fracture surfaces, the joints (if one or more sets are suitably oriented), and finally the lower resistance of faults or clay-filled discontinuities.

10 REFERENCES

Bandis, S. C., Lumsden, A. & Barton, N. 1981. Experimental studies of scale effects on the shear behaviour of rock joints. *Int. J. of Rock Mech. Min. Sci. and Geomech. Abstr.* 18, 1-21.

Bandis, S. C., Lumsden, A.C. & Barton, N. 1983. Fundamentals of rock joint deformation. *Int. J. Rock Mech. Min. Sci. and Geomech. Abstr.* Vol. 20: 6: 249-268.

Bar, N. and N. Barton, 2017. The Q-slope method for rock slope engineering. *Rock Mechanics and Rock Engineering. Springer (2017)* 50: 3307-3322.

Barton, N. 1971. *A model study of the behaviour of steep excavated rock slopes. Ph.D. Thesis*, Univ. of London.

Barton, N. 1971. Progressive failure of excavated rock slopes. *13th US Symp. of Rock Mech. Stability of rock slopes, Illinois,* 139-170.

Barton, N. 1973. Review of a new shear strength criterion for rock joints, *Engineering Geology, Elsevier, Amsterdam,* Vol. 7, 287-332.

Barton, N. & Hansteen, H. 1979. Very large span openings at shallow depth: Deformation magnitudes from jointed models and F.E. analysis. *4th RETC; Atlanta Georgia,* Vol. 2: 1131-1353. Eds Maevis and Hustrulid. *Am. Inst. of Min. &, Metall., and Petr. Engrs, Inc. New York.*

Barton, N. 1982. Modelling rock joint behaviour from in situ block tests: Implications for nuclear waste repository design. *Office of Nuclear Waste Isolation, Columbus, OH,* 96 p., ONWI-308, September 1982.

Barton, N., Bandis, S. & Bakhtar, K. 1985. Strength, deformation and conductivity coupling of rock joints. *Int. J. Rock Mech. & Min. Sci. & Geomech. Abstr*. 22: 3: 121-140.

Barton, N. 1986. Deformation phenomena in jointed rock. 8th Laurits Bjerrum Memorial Lecture, Oslo. *Geotechnique,* Vol. 36: 2: 147-167.

Barton, N. 1993. Physical and discrete element models of excavation and failure in jointed rock. Keynote lecture, *ISRM Int. Symp. on Assessment and Prevention of Failure Phenomena in Rock Engineering,* 5-7 April, Istanbul, Turkey.

Barton, N., By, T.L., Chryssanthakis, P., Tunbridge, L., Kristiansen, J., Løset, F., Bhasin, R.K., Westerdahl, H. & Vik, G. 1994. Predicted and measured performance of the 62m span Norwegian Olympic Ice Hockey Cavern at Gjøvik. *Int. J. Rock Mech, Min. Sci. & Geomech. Abstr*. 31:6: 617-641.

Barton, N. 1999. General report concerning some 20th Century lessons and 21st Century challenges in applied rock mechanics, safety and control of the environment. *Proc. of 9th ISRM Congress, Paris,* 3: 1659-1679, Balkema, Netherlands.

Barton, N. 2002. Some new Q-value correlations to assist in site characterization and tunnel design. *Int. J. Rock Mech. & Min. Sci.* Vol. 39/2:185-216.

Barton, N. 2007. Near-surface gradients of rock quality, deformation modulus, Vp and Qp to 1km depth. *First Break, EAGE*, October, 2007, Vol. 25, 53-60.

Barton N. 2011. From empiricism, through theory, to problem solving in rock engineering. *ISRM Cong., Beijing. 6th Müller Lecture. Proceedings. Harmonising Rock Engineering and the Environment,* (Qian & Zhou ed), Beijing Taylor & Francis, (1):3-14.

Barton, N. and S.K. Pandey, 2011. Numerical modelling of two stoping methods in two Indian mines using degradation of c and mobilization of φ based on Q-parameters. *Int. J. Rock Mech. & Min. Sci.*, 48,7: 1095-1112.

Barton, N. 2013. Shear strength criteria for rock, rock joints, rockfill and rock masses: problems and some solutions. *J. of Rock Mech. & Geotech. Engr.*, Wuhan, Elsevier 5(2013) 249-261.

Barton N and N. Bar. 2015. Introducing the Q-slope method and its intended use within civil and mining engineering projects. In Schubert & Kluckner (ed.), *Future Development of Rock Mechanics; Proc. ISRM symp. Eurock 2015 & 64th Geomechanics Colloquium,* Salzburg: 157-162.

Barton, N.R. and S.C. Bandis, 2017. Characterization and modelling of the shear strength, stiffness and hydraulic behaviour of rock joints for engineering purposes. *Rock Mechanics and Engineering,* Ed. Xia-Ting Feng, Vol. 1, Principles. Ch. 1, 3-40. Taylor & Francis.

Barton, N. and Shen, B. 2017. Extension failure mechanisms explain failure initiation in deep tunnels *and* critical heights of cliff faces and near-vertical mountain walls. *US Rock Mech. Symp. San Fransisco,* ARMA17-686, 20p.

Barton, N. 2021. New ideas about failure modes in rock masses – from tunnels to Prekestolen to El Capitan to Everest. *Bergmekanikkdag,* Oslo. 33.1-33.20.

Bieniawski Z.T. 1989. *Engineering Rock Mass Classifications: A Complete Manual for Engineers and Geologists in Mining, Civil, and Petroleum Engineering*, New York, Wiley, 272p.

Carranza-Torres, C. 2021. Computational tools for the analysis of circular failure of rock slopes. Keynote Lecture. *In Proceedings of EUROCK 2021. Mechanics and Rock Engineering from theory to practice.* Turin. Italy.

Chryssanthakis, P., Monsen, K. & Barton, N. 1991. Tunnelling in jointed rock simulated in a computer. (In Norwegian*). Tunneller og Undergrunnslanlegg,* 1989-1991, NTNF, Oslo, pp. 23-28.

Hajiabdolmajid,V., C. D. Martin and P. K. Kaiser, 2000. Modelling brittle failure. *Proc. 4th North American Rock Mechanics Symposium, NARMS 2000* Seattle, J. Girard, M. Liebman, C. Breeds and T. Doe (Eds), 991–998. Balkema.

Hoek. E. and J. Bray, 1974. *Rock slope engineering*. Institute of Mining.

Hoek, E, C. Carranza-Torres & B. Corkum, 2002. Hoek-Brown failure criterion – 2002 Edition. *Proc. NARMS-TAC Conference,* Toronto, 2002, 1, 267-273.

Lorig, L., P. Stacey and J. Read 2009. Slope design methods, *Ch 10 in Guidelines for Open Pit Slope Design,* Eds. Read and Stacey, CSIRO Publishing.

Martin, C. D. and P. F. Stacey, 2013. Pit slopes in weathered and weak rocks. *Slope Stability 2013.* Brisbane. P. M. Dight (ed), Australian Centre for Geomechanics, Perth, 29p.

Patton, F. D. 1966. Multiple modes of shear failure in rock. *Proc. 1st Cong. of Int. Soc. Rock Mech. Lisbon*. Vol. 1, 509-513.

Potvin, Y. 1988. *Empirical open stope design in Canada*, Ph.D. thesis. Univ. of British Colombia, Canada, 350p.

Renani, H.R. and M. Cai, 2021. Forty-Year Review of the Hoek–Brown Failure Criterion for Jointed Rock Masses. *Rock Mechanics and Rock Engineering* 55(4):1-23.

Shen, B., O. Stephansson, and M. Rinnie, 2013. *Modelling Rock fracturing Processes – A Fracture Mechanics Approach Using FRACOD.* Springer, 173p.

Styles, T.D. & A. Vakili, 2020. Slope Angle Versus Slope Height - The Basis of an Empirical Tool for Slope Design Within Fractured Rock Masses using IUCM. *EUROCK 2020*, Trondheim

Ván, P. and B. Vásárhelyi, 2014. Sensitivity analysis of GSI based mechanical parameters of the rock mass. *Periodica Polytechnica, Civil Engineering*. 58/4 (2014) 379–386.